

Review

Research Progress of Self-Cleaning, Anti-Icing, and Aging Test Technology of Composite Insulators

Qiang He ^{1,2,*} , Wenjie He ^{1,2}, Fangyuan Zhang ^{1,2}, Yiming Zhao ^{1,2}, Lu Li ¹, Xiangjun Yang ¹ and Fengwei Zhang ^{1,*}

¹ College of Mechanical and Electrical Engineering, Gansu Agricultural University, Lanzhou 730070, China

² College of Civil Aviation Safety Engineering, Civil Aviation Flight University of China, Guanghan 618307, China

* Correspondence: aystar@163.com (Q.H.); zhangfw@gsau.edu.cn (F.Z.)

Abstract: Composite insulators are widely used in power systems because of their advantages of light weight, good pollution resistance, and high mechanical strength. With the increasingly serious environmental pollution problem, especially in winter at high latitudes, composite insulators are easily affected by fog, bird droppings, algae, and icing. Long-term exposure to the outdoor insulator surface will cause aging, which will then pose a potential safety hazard to the stable operation of insulators. Therefore, the self-cleaning, anti-icing, and aging test technologies of composite insulators are particularly important. This paper introduces the research progress and current situation of self-cleaning, anti-icing surface preparation, and aging test technology of composite insulators, and looks forward to the future development of composite insulators.

Keywords: composite insulators; self-cleaning; anti-icing; aging; testing technology



Citation: He, Q.; He, W.; Zhang, F.; Zhao, Y.; Li, L.; Yang, X.; Zhang, F. Research Progress of Self-Cleaning, Anti-Icing, and Aging Test Technology of Composite Insulators. *Coatings* **2022**, *12*, 1224. <https://doi.org/10.3390/coatings12081224>

Academic Editor: Ludmila B. Boinovich

Received: 5 July 2022

Accepted: 12 August 2022

Published: 22 August 2022

Publisher's Note: MDPI stays neutral with regard to jurisdictional claims in published maps and institutional affiliations.



Copyright: © 2022 by the authors. Licensee MDPI, Basel, Switzerland. This article is an open access article distributed under the terms and conditions of the Creative Commons Attribution (CC BY) license (<https://creativecommons.org/licenses/by/4.0/>).

1. Introduction

Insulators are one of the most important components of the power system, and their good operation is essential for the reliable transmission of electrical energy, which supports economic development. Insulators mainly serve two functions: supporting and fixing current-carrying conductors, and forming good insulation between current-carrying conductors and the ground [1]. Ceramic insulators, glass insulators, and composite insulators have appeared, successively. The ceramic insulator is the most widely used insulator in the electric power system. It was first developed with the rise of the electric power industry and has been in use for over 100 years. Tempered glass insulators appeared in the mid-1930s. They were made in England using the tempering procedure, and have been widely used worldwide [2]. However, during long-term operation, because of environmental pollution such as foggy weather [3–5], algae pollution [6–8] (Figure 1h,i [6]), and bird droppings [9,10], pollutants can adhere to the surfaces of insulators (Figure 1e–g [11]), which could reduce the dielectric strength of insulators and lead to fouling and flashing accidents [11]. In order to reduce the occurrence of pollution flashover accidents, researchers began to conduct experimental research on composite materials.

Insulators made of polymers were introduced in the 1940s. The first polymers used in insulator manufacturing were epoxy resins, which have good mechanical and thermal properties and excellent electrical properties [12]. In the late 1960s, composite insulators appeared, which were made of resin-reinforced FRP mandrels, with polymer materials such as rubber or fluoroplastics used as the umbrella skirt sheath. Composite insulators have been running in various test lines and industrial lines in more than 30 countries and regions since the 1980s. Of these many countries, the United States is the country that uses composite insulators most widely. Figure 1a [13] shows an example of a composite insulator.

the twenty-first century. This balance means that it is urgent to achieve carbon neutrality, that is, ensuring the total amount of CO₂ emissions in the whole year is zero [16]. On the road to carbon neutrality, the development of electric power plays a central role in the development of a sustainable future [17,18]. Considering that the power generation and transportation sectors are the two largest sources of carbon emissions in most countries [19], decarbonization of power generation and electrification of transportation sectors (including heavy, air, and sea traffic and light to medium-sized vehicles) are crucial to achieving the target goal of neutrality [20,21]. Therefore, it is very important to integrate more renewable energy and increase it for the future development of power systems. Vigorously developing insulating materials can improve long-distance high-voltage transmission capacity and reduce the loss of electric energy and other energy sources. Additionally, the engineering challenges faced by insulation systems in future power equipment/devices and electrified transportation assets have attracted the attention of scientists who wish to produce environmentally friendly insulating materials that can withstand extreme environments [22].

Among the various types of composite insulators that exist, silicone rubber (SIR) insulators account for the majority. The molecular formula of silicone rubber is shown in Figure 1b [13]. Silicone rubber composite insulators have been extensively applied in power systems because of their light weight, high mechanical strength, and excellent resistance to damage and pollution [23]. The strong hydrophobic properties of silicone rubber composite insulators are key properties that are effective in suppressing the occurrence of leakage currents [24]. It is the best choice for outdoor insulators in heavily polluted areas [25]. Some studies have shown that the flashover voltage of composite insulators is higher than that of porcelain insulators and glass insulators in polluted areas [26,27]. In recent years, superhydrophobic surfaces have attracted great research interest from researchers because of their potential applications in various engineering fields [28]. With the continuous advancements of materials, science, and bionics, the technology of manufacturing superhydrophobic surfaces has been increasingly developed [29,30]. In order to improve the hydrophobicity of composite insulators, researchers all over the world have started to study the hydrophobic surfaces of composite insulators [13,31–39].

In many countries and regions with frequent blizzards, icing on insulators and transmission lines can easily lead to serious accidents in power systems. Traditional active deicing methods include mechanical deicing, electric deicing, and liquid deicing, etc. These deicing methods have some disadvantages, such as requiring large equipment, large energy consumption, and a complicated process. This makes the passive deicing method, based on anti-icing coating, popular. In recent years, researchers have found that silicone rubber is hydrophobic, and it can also reduce the low adhesion rate of ice on the insulator surface and reduce the degree of icing [34,40,41]. Therefore, the superhydrophobic surface based on the self-cleaning function of lotus leaves is generally considered to be one of the important development directions of anti-icing. This interesting phenomenon has been applied to airplane anti-icing [42] and electric anti-icing systems. It is proven that the hydrophobic property of superhydrophobic surfaces causes supercooled water droplets to bounce off the surface and reduces the nucleation probability of supercooled water vapor. The coalescence of condensed water droplets promotes the spontaneous bounce of water droplets off the surface, and the air pockets in thousands of micronanostructures on the surface reduce the heat transfer efficiency [43]. The above phenomenon can effectively delay icing, as well as reduce icing area and icing weight, thus bringing good anti-icing performance to a superhydrophobic surface. Even after freezing, the joint position between the micronanostructure and the ice layer is the basic point of microcrack initiation, and the local stress amplification significantly reduces the adhesion strength of ice. Under the action of external forces such as wind, self-gravity, vibration, or an external force field, the ice is easily detached from the surface to achieve the purpose of easy deicing, to enhance the deicing ability of a superhydrophobic surface [44]. Nowadays, more and more insulators with superhydrophobic and anti-icing properties are being introduced which solve the pollution flashover problem

and the icing problems of insulators. With the further research of scientists in the future, additional kinds of insulators will be used in high-voltage transmission.

However, silicone rubber composite insulators are made of organic materials. Under the interaction of strong electric fields, air corrosion, ultraviolet radiation, fouling, and rainwater, the surfaces of composite insulators will age (Figure 1k–m [11]), resulting in reduced hydrophobicity [45,46], and consequently, severe pollution flashover of transmission lines [47]. At the same time, it will also result in insulator depolymerization, tracking, erosion, and reduction of dielectric and mechanical strength [48,49]. The reliability of outdoor composite insulators is imperative for safe circuit operation. Therefore, it is necessary to detect the aging of composite insulators accurately and quickly. Composite insulator detection technology is constantly developing, from the traditional detection methods of a single index such as hydrophobicity, scanning electron microscope, thermal stimulation current, nuclear magnetic resonance, Fourier transform infrared spectrum, X-ray photoelectron spectrum, photothermal radiation, etc., to the modern intelligent testing technology method of multi-index fusion. In the future, it will develop towards more accurate and convenient testing technology.

This paper analyzes and collates many research developments on composite insulators both at home and abroad. The research progress of composite insulators is summarized and prospected from the aspects of preparation of hydrophobic coating, anti-icing methods, and aging of composite insulators.

2. Environmental Impact on Insulators

2.1. Fog Environments

In low temperatures, cold fog will form water droplets or even freeze on the insulator surface. Then, the insulator will corona and aggravate the surface hydroxylation. The surfaces of insulators will generate acidic substances such as nitric acid and produce cracks [3], which will accelerate the aging of insulators. Insulators exhibit more intense AC corona activity in acidic foggy environments than in conventional foggy environments. Acidic fog will not only introduce acidic substances such as nitric acid into the composite insulator to affect the performance of the insulator, but also intensify the oxidation and hydroxylation on the surface of the composite insulator, leading to the reduction of hydrophobicity of the composite insulator. Zhang, Z. et al. [5] applied direct current (DC) voltage to silicone rubber composite insulators for salt spray testing. Through the test, it was found that many pores appeared on the surface of silicone rubber composite insulator in a salt spray environment, which leads to the increase of surface roughness and the decrease of hydrophobic property, as shown in Figure 2a,b [5]. Salt fog also causes the flashover voltage of composite insulators to decrease. With the accelerated developments of industry and urbanization, haze is becoming more and more frequent. This poses a new threat to the safety of outdoor insulators. Over an extended duration of time in the haze, outdoor insulators will become contaminated by haze particles. The contaminated layer attached to the insulator surface becomes moist, and soluble pollutants dissolve in water, which will lead to the formation of a conductive layer and accelerate the generation of a leakage current. Even under some conditions, insulators will flashover [25,50–53], which seriously endangers the normal operation of insulators.

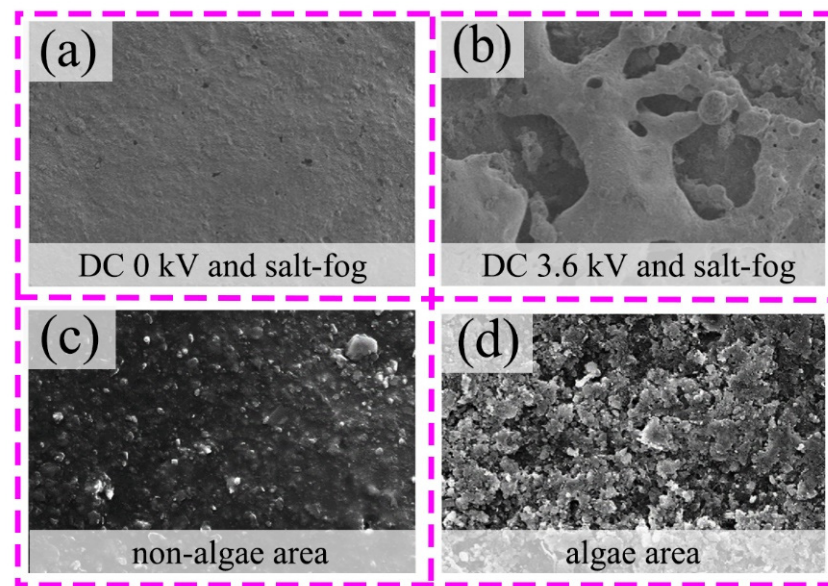


Figure 2. Electron microscope image of an insulator after environmental pollution. (a,b) Electron microscope diagrams of 0 KV, 3.6 KV insulator in a salt fog environment. (c,d) Electron microscopic comparison of insulators before (c) and after (d) algae pollution.

2.2. Algae Pollution

In some countries with tropical and subtropical climates, the humidity is more suitable for algae growth. Algal organisms are mainly green algae, the growth of which can lead to reduced or even destroyed hydrophobicity. Studies have shown that the flashover voltage of algae-covered insulators is 25.2%–41.8% lower than that of clean insulators. The surface of silicone rubber insulators is more conducive to algae growth than ceramic materials. Thus, the composite insulator surface cannot resist algae contamination, which can pose a potential threat to the safe operation of the power system.

Ouyang, X. et al. [7] studied the influence of algae pollution on composite insulators. The algae-covered insulators were compared with the clean insulators under a scanning electron microscope (SEM). It was found that the algae-covered areas showed various degrees of damage such as dents and cracks, and the surface became rough and granular, as shown in Figure 2c,d [7]. Algae are hydrophilic organisms. The hydrophobicity of the surface of the algae-covered insulator will continue to decrease with the growth of algae on the surface, and eventually tend to 20° stable, from a hydrophobic to a hydrophilic state. Algae have a great influence on insulators; the removal of algal contamination from insulators has become an important research topic. Ouyang et al. added antibacterial aerogel to room-temperature vulcanized (RTV) coating, and then sprayed it on an insulator with plasma. These experiments reveal that the coating can effectively inhibit the growth of algae. At the same time, it is very important to effectively detect the degree of algae contamination on composite insulators during actual operation. In the literature [8], this degree of contamination can be determined through image pre-processing, image color segmentation, image morphology operation, and parameter calculation, which allows the extraction of the contaminated area and calculation of the algae coverage percentage for the taken composite insulator pictures. In the future, we are hopeful that there will be more solutions for algae pollution to advance the continuous development and progress of composite insulators.

2.3. Pollution from Bird Droppings

In the process of power system operation, bird droppings will bring fatal harm to power transmission lines and guano flashover as the most important type of bird damage, accounting for more than 90%, which has always attracted the attention of researchers.

Peng, K. et al. [9] have studied bird droppings flashover in tropical China and found that when the water content of bird droppings is low, the flashover probability of the insulator bird droppings surface is much higher than that of accumulated pollution flashover, but when the water content of bird droppings is high, the flashover probability of bird droppings is essentially the same as that of accumulated pollution flashover. Liu, S. et al. [10] found that bird droppings flashover of composite insulators mainly occurs in environments with high humidity and low temperatures in the early mornings, because the hydrophobicity of silicone rubber composite insulators polluted by bird droppings will decrease with the decrease of ambient temperature, and the hydrophobicity recovery time will be longer.

The flashover accident of insulators caused by falling bird droppings can essentially be divided into the following situations. One situation is that when large birds defecate from the low-voltage end of an insulator, the air gap around the insulator string distorts the electric field near the insulator string at the moment of bird defecation, which leads to breakdown. The other situation is that the sparse bird droppings pour onto the surface of the insulator. When the quantity of bird droppings is particularly large, it can even short-circuit the skirt of the insulator and lead to flashover along the surface of the insulator string. The other outcome is that bird droppings accumulate in the same insulator string for a long time, and dry bird droppings and wet bird droppings are mixed, which will lead to flashover discharge in case of wet weather. Bird droppings pollution seriously affects the normal operation of the electric power system. In order to prevent bird droppings pollution, people have taken many measures, such as setting up bird repellents like pulse repellents, sound repellents, and ultrasonic bird repellent facilities. Composite insulators can also be used. The superhydrophobic nature of the composite insulator makes bird droppings less likely to fall on the insulator, reducing the harm caused by bird droppings to the insulator.

2.4. The Low Temperature Effect

In cold climate areas, besides being polluted, the insulator surface will also freeze. Ice accumulation on electrical equipment can be caused by ice fog, heavy snow, or frost. Ice accumulation on transmission lines and insulators often leads to line trips, line breaks, tower failures, insulator flashovers, and communication interruptions, causing huge economic losses in many countries [54,55]. The performance of outdoor insulators under ice and snow conditions is a great concern for power companies.

Common anti-icing methods include mechanical deicing, current deicing, and robotic deicing. However, certain methods can fundamentally solve the problem of insulator icing. One such method is to spray RTV or modified RTV coating on glass or ceramic insulators to achieve the anti-icing effect. The other is to directly manufacture the anti-icing insulator. Studies have shown that hydrophobicity can inhibit the formation of ice by weakening the adhesive force between ice and the insulator surface. By preparing a composite insulator surface with both superhydrophobic and anti-icing effects, it is possible to achieve both self-cleaning effects and delayed icing time.

3. Self-Cleaning Technology for Composite Insulators

Superhydrophobic surfaces are derived from nature's organisms. Lotus enjoys the reputation of "lotus unsullied from mud, wash clean without demon." Many micronano-structured protrusions were observed on the lotus's surface after being magnified by a scanning electron microscope. It is these bulges that make the lotus surface super-hydrophobic and play a role in cleaning surface dust. Some insects have very small superhydrophobic structures on their feet that allow them to fly on a lake surface without cutting the water surface. Superhydrophobic surfaces have attracted the research interest of scientists in recent years due to their potential applications in various engineering fields [56–60]. With the continuous development and maturing of material science and bionic science, modern scientists have prepared bionic superhydrophobic materials through research. A material surface contact angle greater than 90° is a hydrophobic surface. When the

contact angle of the material surface is greater than 150° and the rolling angle is less than 10° , the surface is superhydrophobic. Superhydrophobic surfaces can not only improve the waterproof performance of materials, but also improve the self-cleaning ability and anti-pollution abilities of materials. At present, there exist two ideas for the preparation of a superhydrophobic surface. One is to build a rough micronanostructure on the surface of the material with low surface energy, and the other is to add a low surface energy material modification on the rough surface. The existing mature preparation methods of superhydrophobic materials include the etching method [61,62], template method [63,64], spraying method [65,66], solution soaking method [67–69], sol-gel method [70], electro-spinning method [71,72], electrochemical deposition method [73,74], and phase separation method [75], among others.

During operation, insulators encounter contaminants such as dust, algae, and bird droppings, which are soluble and insoluble contaminants that can adhere to the insulator surface. These pollutants in the rain and fog make the pollutants wet and causes them to dissolve in water, forming a conductive layer, which causes pollution flashover and serious accidents. The use of composite insulators has countered this problem effectively. The hydrophobicity and hydrophobicity recovery given by silicone rubber is a key property [76] which can stop pollutants from adhering to the insulator surface and prevent pollution flashover accidents. Some studies have also reported the flashover performance of superhydrophobic coatings, showing the increase of flashover voltage and the decrease of leakage current [32,77,78]. Many researchers are beginning to devote their efforts to modifying composite insulators to a superhydrophobic state to improve their fouling resistance. At present, the commonly used preparation methods of superhydrophobic surfaces of composite insulators mainly include laser engraving, template method, coating method, spraying method, and mixing method, among others.

3.1. The Laser Engraving Method

Laser engraving is the simplest and most effective method for the surface modification of silicone rubber. One benefit is that it will not change the performance of the silicone rubber itself. The microstructure with a hydrophobic effect is carved directly onto the surface of the insulator by laser engraving, so that the insulator can achieve a hydrophobic effect.

Kietzig, A.-M. et al. [79] took inspiration from the dual-scale roughness structure of the lotus flower surface and sculpted it using a femtosecond laser (CoherentMira HP, CoherentMira, Santa Clara, CA, USA). It was found that various materials changed from the initial superhydrophilic state to superhydrophobic state, and the contact angle became about 150° . Ta, D.V. et al. [80] proposed that infrared nanolaser (20W EP-S) offers a lower cost and more powerful capabilities to sculpt textures, with a steady-state contact angle of 152° . Wu, B. et al. [81] proposed a microstructuring of stainless steel surfaces by irradiating the samples with femtosecond laser pulses and using surface silanization. The prepared stainless steel surfaces with micron and submicron dual-scale structures achieved a maximum contact angle of 166.3° and a roll angle of 4.2° . Yan, Z. et al. [82] proposed a method to create nanostructured micropit holes on the surface of mold steel using a high-power picosecond laser (Edgewave, Germany) coupled with a high-speed scanning mirror (Scanlab HurrySCAN II 14, Scanlab, Germany). The die was directly applied to the vulcanization process of silicone rubber to make the prepared silicone rubber superhydrophobic.

Zhao, M. et al. [13] used a laser engraving machine (D80M) to engrave nine different textural patterns on the silicone rubber surface: with square column (SC), square hole (SH), circular column (CC), circular hole (CH), transverse groove (TG) where the direction of the groove was perpendicular to the umbrella skirt angle, vertical groove (VG) where the direction of the groove was parallel with the umbrella skirt angle, oblique groove (OG) where the direction of the groove was at a 45° angle from umbrella skirt, corrugate groove (CG), and diamond column (DC) with an acute angle of 60° , as shown in Figure 3 [13]. Experiments have shown that the diamond column (DC) with an acute angle of 60° is the

most effective, and the contact angle is increased from 94.75° to 156° . Moreover, the texture has excellent self-cleaning properties, resistance to acid and alkali corrosion, and durability. The texture remains superhydrophobic even after more than 100 wear cycles. Patil, D. et al. [31] also used a similar nanosecond (Nd:YAG) laser method to etch six different patterns found. When the surfaces of the first etching and the second etching overlap by 50%, the self-cleaning effect is optimal, the static contact angle is 159° , and the rolling angle is 3° .

Texture Designs	Square column	Square hole	Circular column	Circular hole	Transverse groove	Vertical groove	Oblique groove(45°)	Corrugated groove	Diamond column
Surface texture									
Surface morpholo									
Contact Angle (CA)	154°	152°	153.5°	151.25°	153.5°	153°	154°	155°	156°
Sliding Angle (SA)	4.3°	6.5°	4.4°	6.25°	4.6°	5.25°	4.35°	4°	3.75°

Figure 3. Influence of different laser engraving structures on hydrophobicity of composite insulators.

The greatest advantage of laser engraving is that the desired micro- and nanostructures can be directly engraved on the surface of composite insulators to achieve superhydrophobic effects. Moreover, the rich and diverse structures of laser engraving provide diverse structural support for insulators in practical applications [83]. Besides, the sculpted micro- and nanostructures are neatly and regularly arranged and have a complete structure, making the structure stable, highly durable, highly resistant to acid and alkali, and less affected by the environment under outdoor operation, and the surface superhydrophobic structure is not easily damaged. However, in the actual production of silicone rubber composite insulators, the laser equipment is expensive. It takes a long time for laser engraving to create a micronanosurface structure on the surface of silicone rubber. These factors have greatly increased the production cost of laser engraving. It is believed that with the maturing of future technology, laser engraving will become a very good preparation method of silicone rubber composite insulators.

3.2. The Template Method

The template method is a way of copying the surface template with micronanostructures and then molding the material surface. Among the materials commonly used to make templates are nickel, steel, bulk metallic glass (BMG), and aluminum [84]. Others have etched the desired micronanostructured surfaces on templates by mechanical processing [85], laser cautery [86,87], photolithography [88], chemical etching [89,90], and anodic oxidation [91–93]. Then, the micronanostructure polymer surface is produced by polymer processing technologies such as injection molding [94,95], injection compression molding [96,97], compression molding [98,99], and hot compression molding [100–102].

Jin, H. et al. [32] used a controlled test method to compare five types of templates with different roughnesses. First, the templates were placed on the raw rubber surface and put into the vulcanizer. Then, the pressure was set to 10 MPa, the temperature was 160°C , and the curing time was 6 min. Finally, the demolding process was carried out. The static contact angle was found to be 153.5° for a superhydrophobic state at a roughness of $14.63\ \mu\text{m}$ under five roughnesses tested. The superhydrophobicity can have a better electric field shielding effect as measured by flash experiment.

Wang, G. et al. [33] used a stainless steel mesh as a template (shown in Figure 4b,c [33]) to fabricate superhydrophobic insulators. First, they put the mixed rubber in the mold and covered the cleaned stainless steel mesh on the silicone rubber. Then, they put it into the vulcanizer (LN-50T, Lina Industrial (Mechanical) Co., Ltd., Dongguan, China) and vulcanized the rubber for 8 min at 2–3 MPa. Then, the vulcanized rubber is cooled to

about 45 °C, and the stainless steel mesh is removed from the surface of the silicone rubber to obtain a superhydrophobic silicone rubber surface, as shown in Figure 4d,e [33]. The production flow chart is shown in Figure 4a [33]. The static contact angle of the tested superhydrophobic surface (HKCA-15, Beijing, China) is $154.5^\circ \pm 1.3^\circ$, and the rolling angle is $10.5^\circ \pm 0.5^\circ$. Further, if the sample is placed in a drying oven at 200 °C for 1 h to cool down to room temperature, the static contact angle can even reach $157.7^\circ \pm 0.3^\circ$ and the rolling angle reaches $8.2^\circ \pm 0.8^\circ$, as shown in Figure 4f [33], and the superhydrophobic effect is improved. The superhydrophobic property was not significantly weakened by subjecting the sample to a 108 h aging test.

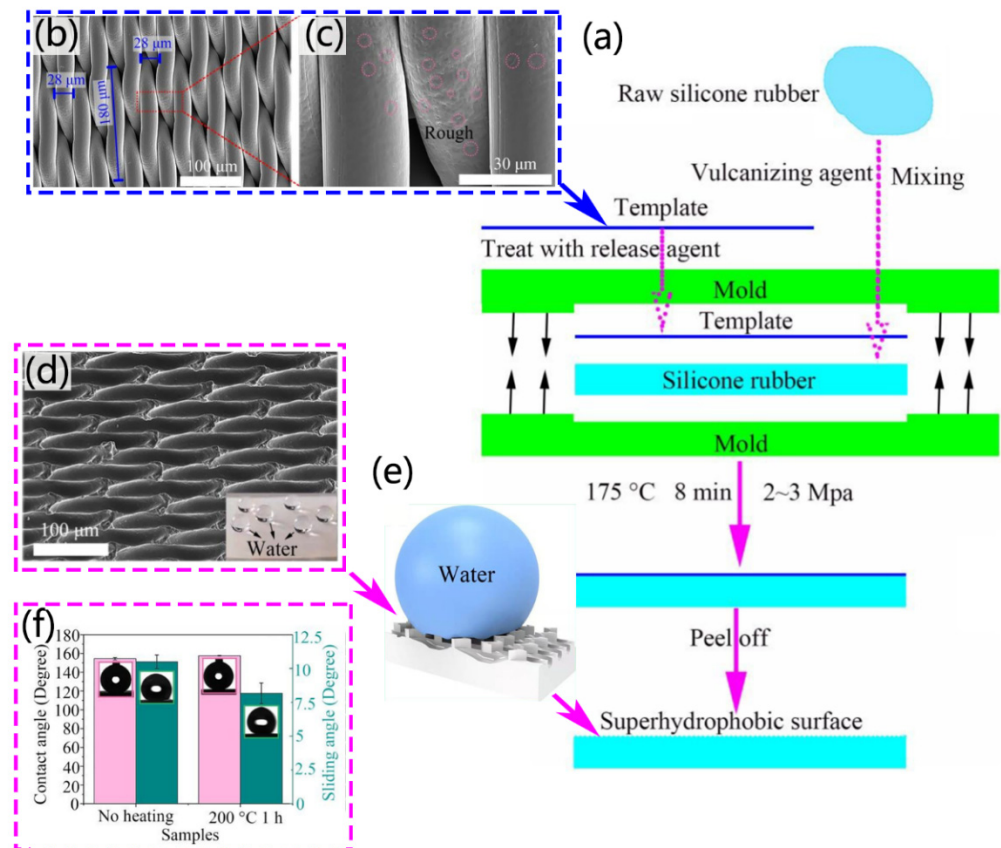


Figure 4. Fabrication of superhydrophobic insulators by template method. (a) Making a flow chart. (b,c) SEM image of a stainless steel mesh template. (d) SEM image of a superhydrophobic insulator. (e) Superhydrophobic model of a composite insulator. (f) Contact angle of a composite insulator.

The material produced by the template method has a stable hydrophobic structure and high durability. Additionally, the template method is simple in the manufacturing process, easy for mass production, green, and pollution-free. The template method is of great significance in the production of silicone rubber composite insulators. This method has been widely used to manufacture micronanostructures on polymer surfaces [103,104] and is widely accepted.

3.3. The Coating Method

At present, the coating method is also a common method to create superhydrophobic surfaces. Seyedmehdi, S. et al. [105] prepared a simple hydrophobic coating by mixing nanofluorine particles with silicone rubber. Allahdini, A. et al. [106] placed the mixture of nanoparticles and organ siloxane on the surface of methyl functional resin as a coating. Ribeiro, A.C. et al. [107] used the mixture of methyl methoxy siloxane and methylsilsesquioxane, loaded with alumina trihydrate and polydimethylsiloxane as the coating, which showed excellent hydrophobic and electrical properties. However, the durability of

the coating structure is weak, and the hydrophobic and hydrophobic migration properties will decrease or even disappear over time. The bonding strength between the coating and the material should be considered when making superhydrophobic coatings using the coating method. In extreme weather environments such as outdoor wind, rainstorms, and blizzard, if the adhesive strength is not strong, the coating will easily fall off or even cause serious accidents. Therefore, when manufacturing superhydrophobic surfaces using the coating method, it is necessary to test the adhesion strength of the coating and other indexes to ensure the normal operation of the composite insulator in practical application.

Li, J. et al. [34] prepared a polydimethylsiloxane (PDMS) and modified nano-SiO₂ hybrid insulator coating. First, they put 3500 mL ethanol solution containing 300 mL ethyl orthosilicate into a flask, and added ammonium hydroxide water into the flask to get gel silica under mechanical stirring. Then, a mixture of 40 mL heptadecafluoro-1,1,1,2-tetrahydro-decyl-1-trimethoxysilane (FAS-17), 40 mL aminopropyltriethoxysilane (APTES), and 40 mL acidic water with pH = 3 was dropped into the flask. The solution was stirred at 60 °C for 6 h and then dried in an oven at 120 °C to obtain modified nanosilica powder. 50 g of hydroxy-terminated poly(dimethylsiloxane) (OH-PDMS), 5 g of dibutyltin dilaurate (DBTD) and 5 g of γ -(2,3-epoxypropoxy)propyltrimethoxysilane (EPTMS) were placed in a flask equipped with a mechanical stirrer. Then they diluted the mixture with 200 mL of 120# solvent oil stirred at room temperature for 10 min. After stirring for 15 min, the resulting mixture was placed in an ultrasonic homogenizer to disperse the nanosilica powder until a homogeneous PDMS/modified nanosilica mixture was obtained. PDMS/modified nano-SiO₂ powder was mixed with 10 g tetrabutyl titanate and 50 mL 120# solvent oil for 5 min under stirring conditions to make a PDMS/modified nano-SiO₂ hybrid mucilage. Finally, the coating was coated on the surface of the insulator and the adhesion reached the highest level through the bonding strength test. Through the contact angle test, the contact angle of the coating is 158°~164°, with an average of 161°, which is a superhydrophobic coating. Through scanning electron microscopy and infrared spectroscopy experiments, it is found that the hybrid coating has a multi-scale microstructure and low surface energy. At the same time, compared with the ordinary RTV coating, the coating not only has good hydrophobicity, but also has the effect of delaying the formation of an ice layer, which can weaken the icing of insulators.

Peng, W. et al. [35] prepared a green and simple superhydrophobic coating of magnesium hydroxide/epoxy resin for synthetic insulators. The stearic acid-modified coating was non-toxic and had low surface energy. The epoxy resin showed high adhesive strength and good bonding ability. First, 2 g of MgCl₆H₂O and 0.1 g of polyvinylpyrrolidone (PVP) were added to 100 mL of deionized water and stirred for 30 min. Then 5 mL of NH₃-H₂O and 45 mL of deionized water were added to the solution and stirred for 2 h at room temperature. Then 0.285 g of stearic acid and 30 mL of ethanol were added to this solution and stirred for 3 h. The mixture was dried in a vacuum oven at 100 °C for 5 h. The white modified magnesium hydroxide particles were collected by filtration and washed twice with ethanol to obtain a superhydrophobic powder. The composite insulator was then immersed in a mixture of 0.23 g of hardener and 0.8 g of epoxy resin for 2 min at room temperature. Then, the modified magnesium hydroxide powder was carefully applied to the coating by dip coating and sieve deposition. Next, the coating covered with white particles was dried in a vacuum oven at 100 °C for 3 h. Finally, the samples were pressed to improve bond strength. The coating exhibited not only excellent superhydrophobicity, low adhesion, and roughness, but also multifunctional properties such as anti-voltage, self-cleaning, anti-fouling, anti-icing, mechanical durability, and chemical stability. Importantly, the obtained MgOH/epoxy superhydrophobic coating can reduce electrical losses and meet the needs of the power industry.

The advantages of the coating method are wide application range and strong universality. The prepared superhydrophobic coating can be used on the surfaces of various materials to achieve a superhydrophobic effect. However, periodic maintenance, such as cleaning and recoating, is required to ensure the continued effectiveness of the coating. In

harsh environments, such as high temperature and heavy pollution, frequent maintenance is even more necessary [106]. At the same time, the adhesive strength and durability between the coating and the material should also be considered.

3.4. The Spraying Method

The spraying method is a common method used to make superhydrophobic surfaces. Generally, spraying a layer of hydrophobic particles onto the surface of materials can achieve a hydrophobic effect. Caldona, E.B. et al. [108] mixed nanoparticles into rubber-modified polybenzoxazine. Spraying it onto the surface of the material bestows hydrophobic and oleophobic effects. Hydrophobic particles sprayed by the spraying method should have good binding force with the surface of the material. Mendoza, A.I. et al. [66] uniformly sprayed zinc oxide with hydrophobic properties onto the surface of the material. When PDMS is used as a substrate, it can obtain more uniform particle distribution and show excellent hydrophobic properties.

Li, Y. et al. [36] created a superhydrophobic surface using the spraying method. First, they poured the liquid vulcanized silicone rubber into a mold and cured it at room temperature for 24 h. Then a 4:1:0.2 mixture of ethyl acetate, one-component liquid silicone rubber, and 30 nm diameter silica particles was mixed under magnetic stirring. After stirring evenly, they sprayed the suspension on the silicone rubber sheet, and cured it at room temperature for 24 h to obtain the superhydrophobic silicone rubber sample. By measuring the static contact angle, the silicone rubber can be improved from 110.7° to 161.8° to reach the superhydrophobic state, and the flashover phenomenon of silicone rubber insulators can be suppressed in the hydrophobic state.

Lei, S. et al. [37] used the spraying method by spraying octadecyltrichlorosilane (OTS)-modified silica nanoparticles onto silicone rubber composite insulators. First, 10 g of silica nanoparticles was added to 100 mL of ethanol with magnetic stirring for 10 min. Then, 100 μ L of OTS was quickly added to it and stirring was continued for 30 min, and the silica particles were separated by centrifugation. The modified OTS was obtained by vacuum-drying at 60°C for 2 h. The strontium, tetraethoxysilane, and OTS-modified SiO_2 particles used were dispersed in hexane and mixed for 2 h. The mixing was continued by adding an appropriate amount of dibutyltin dilaurate catalyst. Finally, the mixture was sprayed and cured overnight at room temperature. The static contact angle was measured to be $165.5^\circ \pm 2.7^\circ$ and the rolling angle was $5.3^\circ \pm 2.4^\circ$, which rendered a good hydrophobic effect.

The greatest advantage of the spraying method is that superhydrophobic surfaces can be obtained quickly and simply. However, the coating is sprayed on the material surface and the sprayed nanoparticles can easily detach due to interactions with the external environment, which is worth considering to ensure the durability of hydrophobic surfaces. Additionally, attention should be paid to the uniformity of sprayed particles during spraying. If the spraying is not uniform, it will lead to uneven hydrophobic properties on the surface of the material.

3.5. The Mixing Method

All of the above methods are commonly used to prepare superhydrophobic composite insulators. In order to achieve a better superhydrophobic effect, studies also exist combining different preparation methods to manufacture superhydrophobic surfaces. Although the fabrication steps are more tedious, the hydrophobicity of the superhydrophobic surface can be further improved through this procedure.

Vallabhuneni, S. et al. [38] fabricated superhydrophobic surface structures by the template method and the spraying method. PDMS sheets were fabricated from 184 siloxane elastomeric substrates and crosslinkers at 10:1, and PDMS solutions were poured onto smooth Petri dishes. The plates were silanized with heptadecafluoro 1,1,2,2-tetrahydrodecyltrichlorosilane on 120-grit and 60-grit sandpaper, cured at 70°C for 90 min, and peeled from the surface. A nanosilica suspension dispersed in hexane was sprayed 15 cm away from its surface. It was

then placed in a vapor-phase silanization chamber at 120 °C for 45 min with 200 μ L of heptadecafluoro 1,1,2,2-tetrahydrodeoxytrichlorosilane to impart a lower solid surface energy, and the experimental flow diagram is shown in Figure 5a [38]. After testing the contact angle, it was found that the sprayed nanosilica particles would change the surface from originally hydrophobic to superhydrophobic, and the surface sandpapered and polished was of better quality than the unpolished sprayed micronanosilica particles.

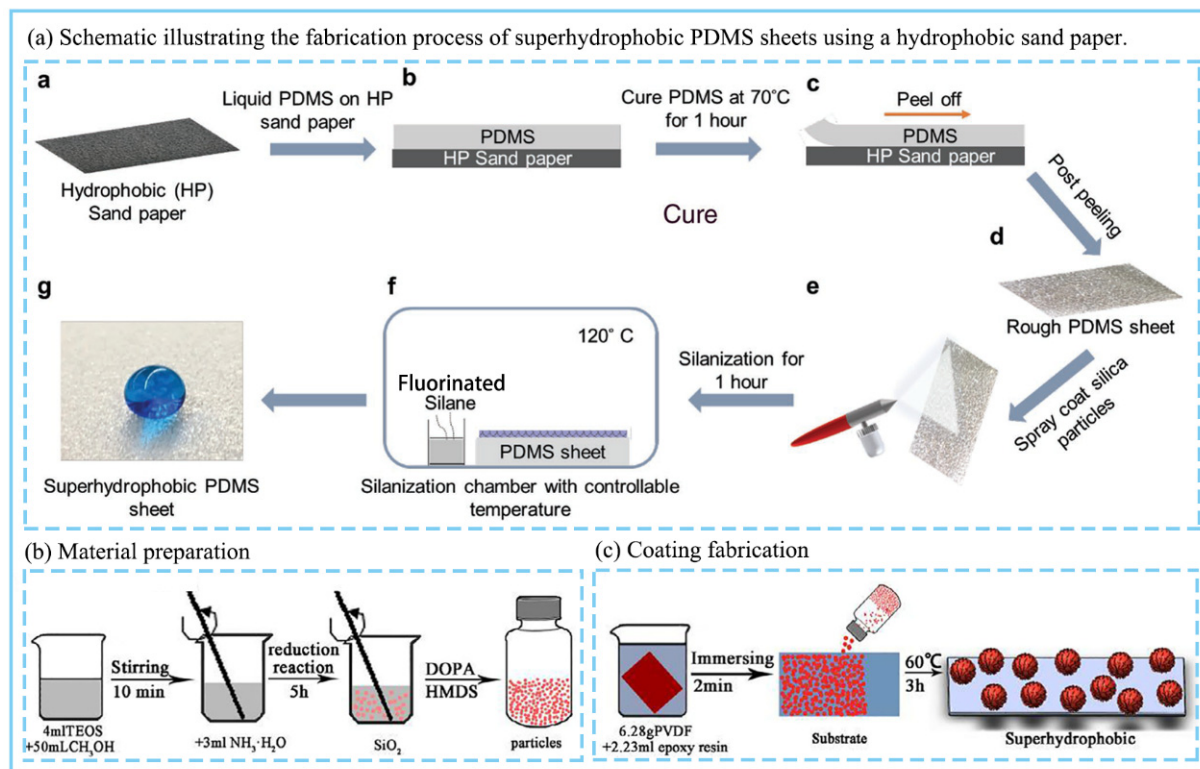


Figure 5. Flow chart for the preparation of superhydrophobic surfaces and the preparation of anti-icing surface coatings. (a) Flowchart of superhydrophobic PDMS sheets using hydrophobic sandpaper. (b) Preparation of superhydrophobic HMDS-dopa silica powder. (c) Flow chart of coating preparation.

Yan, Z. et al. [39] prepared a superhydrophobic structure using the template method and the coating method. First, a template processed with picosecond laser (Edgewave, Germany) covered the surface of silicone rubber to produce a silicone rubber with a micro-nanostructure. Then, the hydrophobic coating was obtained by modifying hydrophobic silica nanoparticles with alkyl fluoride silane and was applied to the surface of the silicone rubber. The obtained nanostructured surface had a static contact angle of 148.2° and a sliding angle of 4.9°.

In the preparation of superhydrophobicity, the contact between continuous dripping water droplets and the surface of the sample has a great influence on the hydrophobicity of the sample. It has been found that hydrophobic materials will interact with water directly. During the use of composite insulators, water molecules will be embedded in the polymer matrix. Long-term contact between a hydrophobic surface and an aqueous medium will lead to the decrease of hydrophobicity. Pashinin, A.S. et al. [109] found that the surface resistivity of superhydrophobic materials decreased when they were exposed to humid atmospheres with the formation of water films. This will affect the normal operation of composite insulators. Boinovich, L.B. et al. [110] treated the sample surface using a femtosecond laser (Amplitude Systèmes, city, Bordeaux, France). Then the laser modified sample was exposed to ultraviolet-ozone treatment. Then, the texture was treated with a hydrophobic solution. It was found that the treated sample still maintained good

hydrophobicity after 20 h, and the contact angle did not change. However, the contact angle of silicone rubber which had not been treated by ultraviolet-ozone decreased very rapidly. Based on research, Emelyanenko, A.M. et al. [111] prepared silicone rubber with texture reinforcement by fluoroxysilane. The change of contact angle between the droplet deposited on the sample and the surface in saturated water vapor was measured. The contact angle of the sample increased in the first 2 h, then finally became stable. This shows that the sample has good contact angle stability. It can ensure that the sample keeps good hydrophobicity in an environment of continuous contact with liquid. Therefore, in the process of preparing superhydrophobic materials, the loss of hydrophobicity caused by the long-term contact between the droplets and the sample surface should also be given due attention.

These methods described above are the main preparation methods for creating superhydrophobic insulators at present. Among them, the composite insulator surface prepared by the laser engraving method and the stencil method has good durability and can resist the corrosion of acid and alkali environments. Laser engraving can engrave a rich variety of hydrophobic surfaces and continuously improve the hydrophobic properties of the surfaces. However, the laser engraving equipment is expensive and the production cost is high, which is not easy for mass production, while the stencil method is more suitable for high-volume production. The coating method and the spraying method should carefully consider adhesion and durability with the material. It is believed that with the continuous progress of science and technology and the unremitting work of researchers, more and more concise methods of creating superhydrophobic insulators will appear.

4. Anti-Icing Technology of Composite Insulators

In a cold climate area, the insulator will not only be polluted, but snow and ice will also have accumulated on its surface. The electric power industry is very concerned about the performance of outdoor insulators exposed to snow and ice. Figure 6a [112] shows a power system damaged by heavy snow. When the ice and snow melt, the probability of flashover and outages is high. Researchers have made many efforts to solve the problem of the icing of insulators. In January 1974, a large ice-covered flashover occurred on a 500 KV transmission line in the U.S. [113] In 1998, three consecutive snowstorms in Canada destroyed more than 1000 transmission towers, and cumulatively, more than 1.7 million people suffered a week of power outage [114]. During the 2008 winter storm in China, freezing rain in central China lasted for more than three weeks, causing 218 ice flashes. Many power towers collapsed under the weight of snow, resulting in power outages in 41 cities and counties. In Hunan and Jiangxi provinces, 37% of 500-kilovolt transmission towers were knocked down [115]. A railway line connecting the south to the northern capital of Beijing was paralyzed by heavy snow and freezing temperatures in Hunan Province. It led to the suspension of at least 136 trains, and the Chinese government estimated the damage caused by the storm at about three billion dollars [116]. In the winter of 2015, the city of Tianjin, China was hit by a snowstorm that seriously affected the safe operation of the power grid, which caused 500 kV transmission lines to flash over many times and triggered significant economic losses [117]. Deicing of insulators has always been a frequent concern of researchers. The anti-icing and deicing technology of transmission lines has been well-developed in recent decades. Common deicing methods include thermal deicing, mechanical deicing, and robotic deicing.

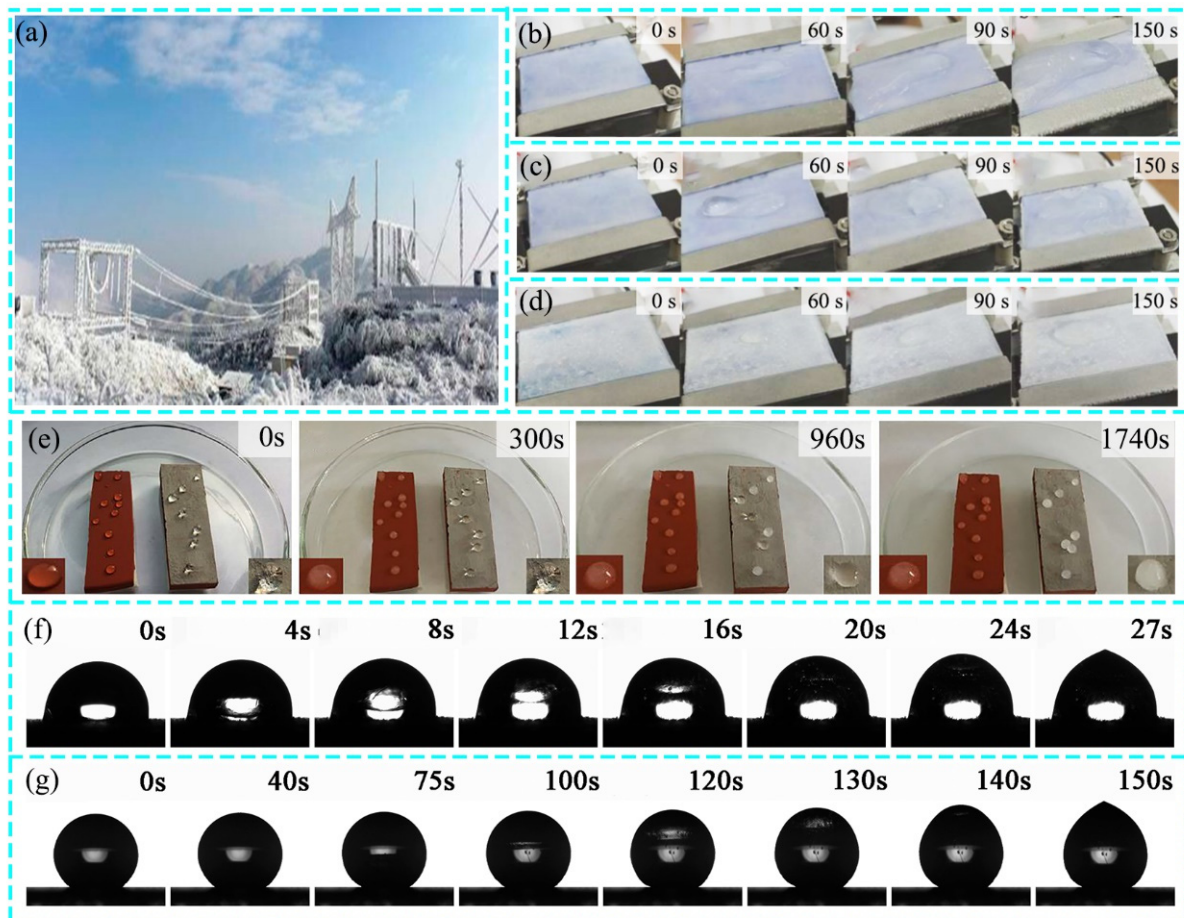


Figure 6. Effect diagram of deicing coating to inhibit icing. (a) A power system is damaged by snow. (b–d) The freezing speeds of hydrophilic, hydrophobic, and superhydrophobic surfaces at 12 °C. (e) Anti-icing test of coated (right) and uncoated (left) composite insulators. (f,g) Water droplets on different surfaces were frozen at 30 °C. (f) HTV silicone rubber. (g) SH coating.

4.1. The Active Deicing Method

The thermal ice melting method, using an additional heat source or self-heating of the wire, makes the ice and snow unable to accumulate on the wire or melts the accumulated ice and snow. The mechanical deicing method serves to remove the snow on the insulator surface by the use of mechanical equipment. The robotic deicing method is a popular deicing method in the last few years, in which robots replace human hands to reach dangerous places where deicing is not easy and automate the operation of deicing. Document [118] introduces a mobile robot for deicing overhead transmission lines. The robot uses a low-voltage DC motor and a lithium-ion battery, which increases the range without increasing the weight of the robot. An arbitrarily expandable wireless transmission module is applied. The electrical control box and battery are specially treated with a new type of waterproof connector. These measures improve the waterproofness of the robot and enhance its reliability. Neural networks were applied to robotic deicing as a promising self-learning control method. Yang, Y. et al. [119] addressed the control problem of a transmission line inspection and deicing robot. First, the mechanical structure and dynamics model of the deicing robot were analyzed. Then, a self-learning control strategy based on neural network was proposed, which consisted of a fuzzy neural network controller and single-layer feedback neural network identifier based on an extreme learning machine (ELM). Yang et al. gave the structure and learning algorithm of the control system and verified the effectiveness of the controller by computer simulation and experimentation. This method saves the manpower traditionally consumed by manual deicing.

The thermal ice melting, mechanical deicing, and robotic deicing methods belong to a group of active deicing methods with the help of external forces. These methods usually require a lot of manpower, complex and dangerous operations, a lot of energy, and expensive equipment consumption, and most of them cannot be used for deicing long-distance power grids [119]. Besides, the irregular shape of insulators hinders the development of automatic deicing devices.

4.2. Passive Deicing Method (Anti-Icing Coating)

In the research of insulator deicing, there are other methods to prevent the formation of ice layer on insulator by adding chemicals such as deicing liquid and salt. Although this method does not require complicated operation, most deicing liquid and deicing salt will pollute the environment and insulators [120]. Therefore, researchers urgently need a method to inhibit the accumulation of ice on insulator surfaces. In this situation hydrophobic anti-icing coating is considered as an effective alternative method for deicing and anti-icing of transmission lines and insulators. This method involves creating a micro-nano structure on the insulator surface or painting a layer of anti-icing material so that water droplets, ice and snow cannot easily cover the insulator surface to achieve a passive anti-icing effect. Compared with traditional deicing methods, the deicing coating can reduce the adhesion rate of ice on the surface, thereby reducing the degree of icing.

Room-temperature vulcanized (RTV) silicone rubber coatings have been widely used in antifouling power grids. The main component of RTV silicone rubber coatings is polydimethylsiloxane (PDMS), which contains $-\text{CH}_3$ groups in its molecular chain and has a certain degree of hydrophobicity. The contact angle of the RTV silicone rubber coating surface is about 110° , and its hydrophobic nature can effectively prevent ice from accumulating on its surface [121]. When the contact angle is greater than 150° and the rolling angle is less than 10° , the superhydrophobicity can allow the water on its surface's near-spherical shape to easily roll off, which prevents the accumulation of ice. Anti-icing of superhydrophobic surfaces has been studied in [122–124], where superhydrophobic coatings can delay icing time and reduce the adhesion of ice.

Lei, S et al. [37] prepared a superhydrophobic coating based on silica nanoparticles and room temperature vulcanized silicone rubber via a simple spraying method. The coating has not only a superhydrophobic effect but also an anti-icing effect. The icing of hydrophilic, hydrophobic, and superhydrophobic surfaces was tested from -4°C to -16°C , and the initial icing times occurred at 30 s, 60 s, and 90 s, respectively, as shown in Figure 6b–d [37]. It is confirmed that the superhydrophobic coating has a strong ability to inhibit ice growth, which can lead to an increase in icing time and reduce the volume of the aggregated ice. At -8°C and -4°C , water droplets rolled away from the cold superhydrophobic surface rapidly. At -12°C , ice accumulation on the superhydrophobic surface is delayed and the ice volume decreases. At -16°C , no anti-icing effect was observed.

Peng, W. [125] et al. produced a green and simple anti-icing coating that can be applied to the surface of composite insulators. First, 4 mL of tetraethoxysilane (TEOS) was mixed with 50 mL of ethanol and stirred for 10 min. Then, 3 mL of $\text{NH}_3\text{-H}_2\text{O}$ was added to the above mixture and stirred for 5 h at room temperature. Subsequently, 0.03 g of 3-hydroxytyramine hydrochloride (dopa) and 8 mL of 1,1,1,3,3,3-hexamethyldisilazane (HMDS) were added to this solution under stirring. After the hydrolysis reaction (TEOS and HDMS), the mixture was dried in a vacuum oven at 100°C for 3 h. The obtained brown HMDS-dopa particles were washed twice with ethanol to obtain this coating as shown in Figure 5b,c [125]. It was found through this experimentation that the composite insulator containing the anti-icing coating required 960 s for the droplets to partially freeze, and about 1740 s to completely freeze at -10°C , as shown in Figure 6e [125]. Altogether, it shows excellent anti-icing performance.

Sun, J. et al. [126] made superhydrophobic coatings using the sol-gel method and plasma spraying. First, 25 mL of Tetraethylorthosilicate (TEOS) and 24 mL of ethanol were mixed with magnetic stirring at room temperature for 30 min, and then 15 mL of nitric acid

solution was added, heated to 70 °C, and stirred for 3 h. Secondly, 2.5 mL of TEOS and 0.25 mL of hydrochloric acid solution were mixed at room temperature for 10 min, and the prepared 2 g of SiO₂ sol and 0.35 g of 1H,1H,2H,2H-Perfluorodecyltriethoxysilane (PDTS) were stirred with a magnetic stirring bar for 1 h. Subsequently, the coating was applied by rotating the coating machine (Chemat Technology, KW-4A) at 500 rpm for 10 s and at 2500 rpm for 2 min. Finally, the prepared coating was sprayed on the insulator surface via plasma spraying. Through the −30 °C icing test, it was found that the icing time of the surface treated with the superhydrophobic coating became 150 s. However, the icing time of the surface of ordinary silicone rubber was 27 s; the treated surface delayed the icing time by 123 s compared with the ordinary surface, as shown in Figure 6f–g [126]. The coating can delay icing and effectively improve the anti-icing performance.

Many studies have also been made on passive deicing. Redondo, O. et al. [127] prepared an anti-icing coating with a self-heating function by adding graphene nanosheets (GNP) in the middle of epoxy resin to achieve some anti-icing and deicing function. However, this method must be applied under high pressure. Chao, Y. et al. [128] prepared ZnO/PDMS composites as superhydrophobic coatings using a simple surface grinding method. This significantly reduced ice accumulation on the surface at very low temperatures (15 °C). Sarra Gam-Derouich, S. et al. [129] first used aryl diazo salts to modify nanostructured copper surfaces, and this low surface energy of the copper substrate led to longer freezing times. Navid Sharif et al. [130] prepared a graded anti-icing microcoating structure using TiO₂. The coating was tested in the icing and deicing cycle, which showed that the coating had sufficient durability. However, there are still some problems in the applications of most coating methods. The stability of the coating material bonded to the substrate, the durability of the coating for reuse, and the high cost of existing anti-icing processes are important issues that affect the practical applications of these methods. [131–133].

Laser engraving is favored by researchers as a way to create durable superhydrophobic and anti-icing properties. Zhao, M. [134] carved on the surface of composite insulator with a laser engraving machine (D80M), selecting laser powers of 15, 25, 35, 45 and 55 W and spacing of 200, 500, 300, 350, 400 and 450 μm. The specimens were found to have the best anti-icing and deicing performance when the power was 35 W and the structure size was 200 μm. This specimen doubled the icing delay time and increased the icing adhesion strength by one-third compared with the original specimen. The advantages of this method are that it is simple to fabricate, can provide good anti-icing and deicing effects on composite insulators, and the surface created by this method is highly durable.

The anti-ice covering method of using superhydrophobic surfaces has a shorter icing time in low-temperature environments. The ice has low adhesion to the surface of the composite insulator, which is easily dislodged by external forces and not easily attached to its surface, reducing the ice coverage on the insulator surface. However, under extreme cold conditions, droplets will easily adhere to the interior of the rough surface. Ice will continue to grow along the bottom of the rough surface structure, even if the rough surface structure is completely covered and its hydrophobic, anti-icing capacity is greatly reduced [135]. To solve this problem, scientists have added photothermal [136], electrothermal [137,138], and magnetothermal [139] plasmas to the coating surfaces to give thermal properties to the conventional superhydrophobic anti-icing surfaces. The combination of active and passive deicing methods greatly improves the anti-icing efficiency of the deicing coating. During the melting process, the thermal effect first causes the ice layer and solid interface to melt into water, and the ice layer is more easily removed. It also reduces the loss of rough structure to improve the durability of the anti-icing coating.

5. Aging Test Technology of Composite Insulators

Although composite insulators have many advantages when compared with glass and ceramic insulators, composite insulators are more prone to aging. This is because composite insulators are composed of organic materials. Organic materials are subject to chemical

changes from environmental influences such as ultraviolet light, temperature environments, cold air, and acidic compounds, resulting in a weakening of the electrical and mechanical properties of composite insulators. Especially for SIR materials, environmental rain, dust, salt, and nitric acid in the air all cause the loss of low-molecular-weight flowing fluid in SIR, the weakening of hydrophobic recovery, and the increasing occurrence of macromolecular chain breakage and even pulverization of SIR [140]. Therefore, aging is a fatal problem for composite insulators.

This necessitates the regular testing of composite insulators. There exist many aging detection techniques for composite insulators. For example, the electrical properties of composite insulators are highly correlated with their degrees of hydrophobicity. Therefore, the hydrophobicity class (HC) and contact angle are used to evaluate aging effect and aging state. The leakage current when the insulator surface is exposed to heavy contamination or moisture for a long time, and the thermal stimulation current (TSC), which characterizes the trap charges and trap levels of composite insulators, are used to evaluate the aging of composite insulators. In recent years, microscopic features of synthetic insulators have been found to be related to the aging process. Images of surface microstructures (obtained by SEM) can characterize the aging states of insulators. Si-CH₃ and Si-O-Si functional groups (measured by Fourier transform infrared spectroscopy (FTIR)) and differences in the elemental composition of composite insulators (measured by X-ray photoelectron spectroscopy (XPS)) are good indicators to characterize the degree of aging of synthetic insulators. The thermal properties of the material are related to the microstructure of the material itself. Thus, the degree of aging of composite insulators can be detected by photo-thermal radiometry (PTR).

5.1. The Hydrophobic Method

The hydrophobicity levels of silicone rubber composite insulators need to be tested periodically [141] to prevent pollution flashover accidents and to improve the reliable operation of transmission lines [142]. The main hydrophobicity testing methods for silicone rubber composite insulators are the static contact angle method, the surface tension method, and the water spray classification method [143]. The static contact angle method requires instrumentation for measuring the contact angle to perform test experiments in the laboratory. Figure 7h is a contact angle measuring instrument [144]. The liquid used for measuring in the surface tension method is harmful to the human body; therefore, it is rarely used in the process of insulator hydrophobicity classification [145]. Water spraying is simple, practical, and economical, but experimental results may vary depending on the experimenter [146]. New efficient inspection methods are emerging with the continuous development of digital imaging and smart grid technologies [147].

Sorqvist, T. et al. [148] studied the long-term performances and aging processes of several types of composite insulators exposed to the environment on the west coast of Sweden, and found a strong correlation between electrical properties and hydrophobicity. The hydrophobicity classification method defined by the Swedish Institute of Transport Research was to observe the state of water droplet aggregation on the insulator surface by means of water spraying. They classified the water droplet aggregation state into seven hydrophobicity classes [149] as shown in Figure 7a–g [150]. Berg, M. [151] et al. developed a numerical image analysis method by introducing the abbreviated average of normalized entropy. This method can provide continuous numerical estimates of hydrophobicity instead of discrete categories. Composite insulators have good hydrophobicity. However, with increasing use, the surface of composite insulators starts to chalk, resulting in a decrease in the hydrophobicity of the insulators.

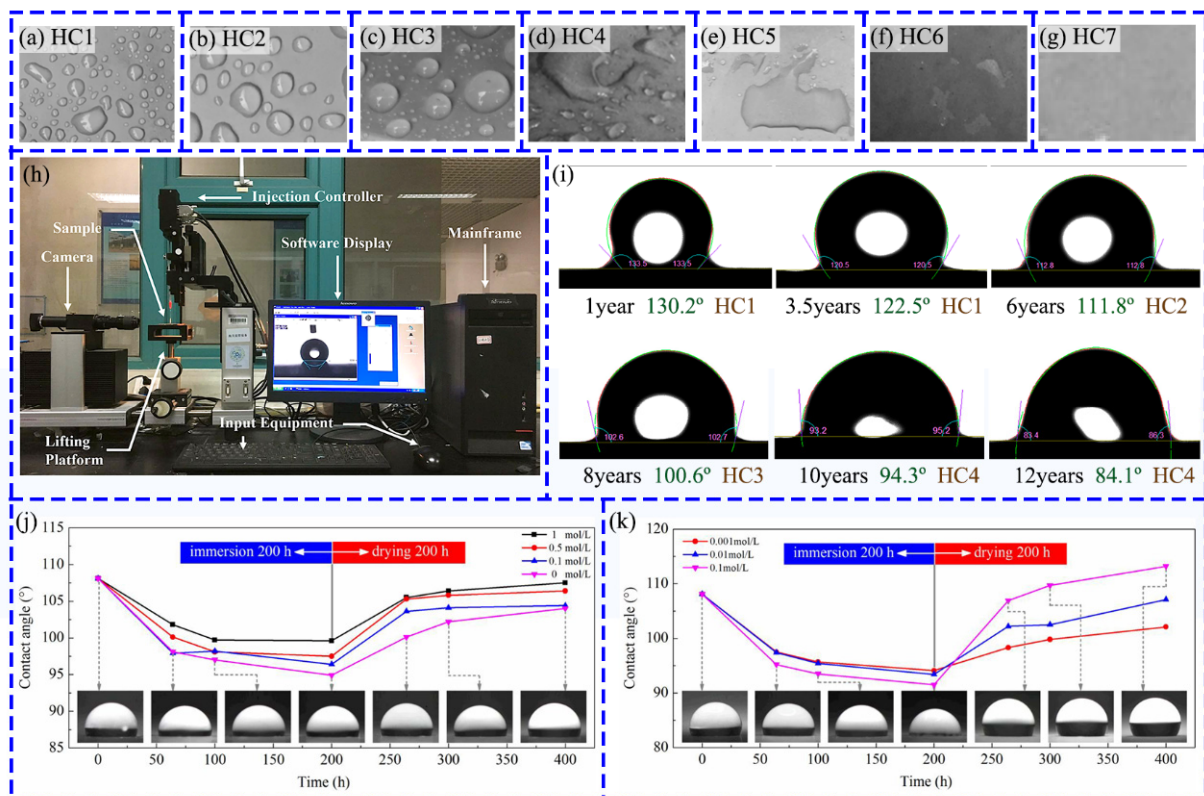


Figure 7. Detection of composite insulator aging by hydrophobic method. (a–g) Comparison diagram of water spray grade method droplets and hydrophobic grade. (h) Contact angle measuring instrument. (i) Contact angle and hydrophobic grade of composite insulators that have been used for 1–12 years. (j) Loss and recovery of hydrophobicity of samples during soaking and drying in NaCl solution. (k) Loss and recovery of hydrophobicity of samples during soaking and drying in nitric acid solution.

Zhang, Y. et al. [112] sampled the composite insulators which had been in operation for 1–12 years at the altitude test station in Hunan province. They measured the contact angle of the sample surface with a contact angle meter (Drop Meter A-100P). The contact angle of the composite insulator after one year of operation was 130.2° , and the hydrophobic grade was HC1. With the increase of running time, the hydrophobic performance of insulators gradually decreases. After 10 years of operation, the contact angle of the insulator was 94.3° , and the hydrophobic grade was HC4, which is still classified as hydrophobic. However, the contact angle of the composite insulators after 12 years of operation decreased to 84.1° . If the contact angle is less than 90° , the material is not hydrophobic. As shown in Figure 7i [112]. Gao, Y. et al. [152] explored the loss and recovery of the hydrophobicity of samples during soaking and drying in NaCl solution, as shown in Figure 7j [152]. The loss and recovery of hydrophobicity of the sample during soaking and drying in nitric acid solution is shown in Figure 7k [152]. These findings reveal that the hydrophobicity of composite insulators will decrease in both salt and acid environments. The hydrophobicity of composite insulators will decrease with the increase of service time. The water spray method is used to measure hydrophobic grade, and a contact angle meter is used to measure contact angle. We can establish a relationship between aging and the hydrophobicity of composite insulators. By testing the hydrophobicity, the aging state of composite insulators can be easily discovered.

Kokalis, C.C.A. et al. [153] introduced a new method for hydrophobicity classification based on convolutional neural networks. The method collected 4500 pictures by spraying water on composite insulators. These pictures were trained, tested, and validated to obtain the water transmission class of the composite insulator. Most of them after experimentation show that the accuracy of this neural network method recognition is close to 98%. This

method can reveal the automatic classification of the hydrophobic grade of insulators, which helps in the aging detection and maintenance of composite insulators.

Hydrophobicity, as an index for evaluating composite insulators, plays an important role in the aging test of composite insulators. The hydrophobicity test is very convenient and quick, especially utilizing the spraying method to measure the hydrophobicity levels of composite insulators. The aging state of the composite insulator can be detected by simply spraying water on it. This method is easy to operate, and does not require complex equipment. With the rapid development of computer neural networks, it is possible to quickly identify hydrophobic grades by training computer neural networks with just one picture. The development of artificial intelligence has laid a solid foundation for the intelligent detection of hydrophobicity.

5.2. The Scanning Electron Microscopy (SEM) Method

A scanning electron microscope (SEM) is a device between a transmission electron microscope and an optical microscope. Scanning electron microscopy allows the observation of the morphology of microstructural surfaces. With its high resolution and magnification, SEM has very wide applications in multiple disciplines, such as physics, material science, and biology. The degree of aging of silicone rubber composite insulators can be assessed by the surface of the sample captured by the scanning electron microscope [154].

Ems et al. [11] aged composite insulators via an artificial polymer aging test. The surfaces of unaged composite insulators, as well as composite insulators aged for 2, 4, and 6 weeks, were photographed using scanning electron microscopy, as shown in Figure 8a [11]. It was found that as the aging progressed, some holes were formed on the insulator surface and the surface gradually became rougher. This causes the hydrophobicity of the composite insulator to decrease, which leads to problems in the operational performance of the insulator. Haddad, G. [155], by comparing the samples under the electron microscope (FEI Quanta 200 SEM, Netherlands), had images taken. He found that the new specimen had a uniform surface with less porosity. The surface roughness and porosity of aged silicone rubber insulators were high and increased with aging time. Zhang, Y. [112] et al. compared the electron microscope (FEI Quanta 200 SEM, Netherlands) images of composite insulators aged for 1–12 years. With the increase of aging time, more and more cracks, dents, and bulges appeared. The surface roughness of the sample increases over time.

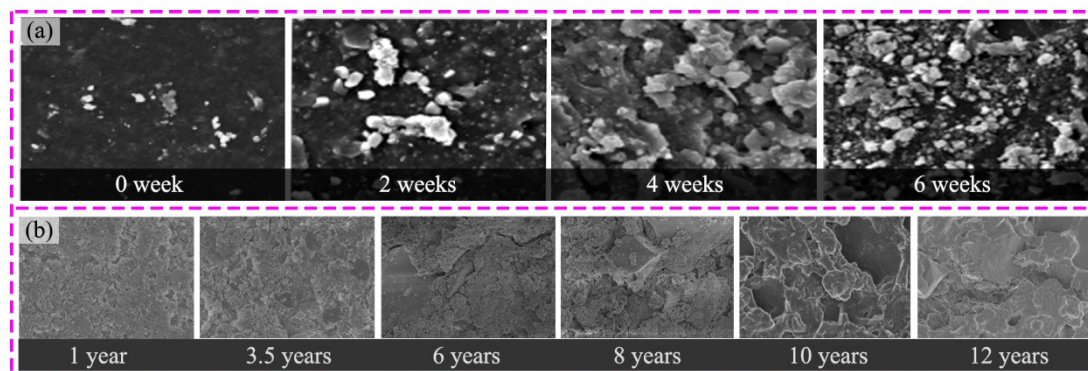


Figure 8. Comparison of aging composite insulators under scanning electron microscope. (a) SEM image of composite insulator after aging for 0 weeks, 2 weeks, 4 weeks, and 6 weeks. (b) SEM image of composite insulator after aging for 1 year, 3.5 years, 6 years, 8 years, 10 years and 12 years.

In summary, with the increase in aging time, defects such as pulverizations, cracks, voids, and dents appear on the surface of silicone rubber composite insulators. A scanning electron microscope (SEM), as a kind of equipment designed to observe the micromorphology of the sample surface, can clearly and intuitively observe the aging state of a silicone rubber surface, reflecting the aging degree of composite insulators.

5.3. The Thermally Stimulated Current (TSC) Method

The thermally stimulated current method is mainly used to measure the microscopic parameters of dielectric materials such as insulators and semiconductors. The aging process of composite insulators may lead to the breakage of molecular chains and the generation of many free radicals, which lead to changes in the internal trap parameters. The increase in trap density can be used as an effective parameter to determine the degree of electrical aging of polymeric materials [156], so the degree of aging of composite insulators can be determined by the thermally stimulated current method. In recent years, TSC has been applied to the study of space charge properties of aged polymers [157–159]. The thermally stimulated current method involves adding a composite insulator between two electrodes in a vacuum environment and heating it to a certain temperature to allow the carriers in it to become excited. Then, a DC polarization voltage is applied to polarize the composite insulator. Immediately afterwards, liquid nitrogen is added to bring the environment down to the lowest possible temperature. When the electrostatics meter reading of the access sample observed decreases to zero with no current passing, the temperature is then increased at an equal rate by observing the relationship of depolarization current to temperature. A thermal stimulus current is a short-circuit current generated by the depolarization of dielectric materials during heating. Generally, this short-circuit current is very small, reaching pA levels.

Ying, L. et al. [160] compared the TSC curves of silicone rubber composite insulators produced by manufacturers A and B and operating during different years. It was found that the TSC curves of the two new samples showed a main peak at 318 K, indicating that the base materials of the composite insulators produced by different manufacturers were essentially the same. Although the TSC curves of manufacturers A and B have some differences, their general curve shapes are similar. This is caused by different material ratios and different vulcanization temperatures and pressures in the production. The peak value of TSC will increase with the increase of service life, and the longer the service life, the more obvious the increase. Ying, L also evaluated the aging state of composite insulators by combining trap characteristics and volume resistivity temperature characteristics. They gave the trap charge rate of change 2.2 as the aging threshold value for sample A. The aging threshold value for sample B was obtained as 2.35. The aging threshold value can help in determining the aging states of insulators.

Zhou, Y. et al. [156] cut the 500 kV AC composite insulator bobbin into four layers longitudinally from the upper surface to the lower surface. The TSC curves were obtained by introducing the thermal stimulation current method into the test. The trap charge of the first layer is less than the other layers, but the trap energy level is the highest. The trap depth of the first layer is deeper than the other layers. The trap level and the number of shallow traps decreases from the second layer to the fourth layer in order. It shows that the aging state of the first layer is more serious than that of the inner layer, and the outermost layer causes the difference in insulator layer aging due to an extended time of fouling and UV radiation.

Tu, Y. et al. [161] used the thermal stimulation current method to test the aging characteristics of silicone rubber composite insulators in three factors: air pressure, relative humidity, and aging time. It was shown experimentally that the effect of pressure on the trap charge was related to both humidity and aging time. The higher the humidity, the greater the trap charge. With the prolongation of low-pressure aging time, the influence of humidity became more obvious. However, as the pressure increased, the effect of humidity on the trap charge gradually decreased. The effect of aging time is more significant, and the aging of silicone rubber deepens as the aging time increases. It is found that the TSC test can reflect the corona aging characteristics caused by physical and chemical defects very comprehensively, so the TSC experimental results can be used as an effective standard for evaluating aging.

The above experiments show that the peak value of the test current increases with the increase of the operating age, and the trap energy level obtained by calculation also

increases. That is, the longer the operating life of the composite insulator, the higher the aging degree, and also the higher the TSC value and trap energy level. Therefore, the TSC can provide some reference for the aging severity level of composite insulators.

5.4. The Nuclear Magnetic Resonance (NMR) Method

The nuclear magnetic resonance (NMR) method is a common method for testing polymer materials. In recent years, NMR technology has been gradually promoted and applied to the study of the aging state of composite insulators. The advantage of NMR is that the equivalent transverse relaxation time of silicone rubber composite insulators can be measured nondestructively. The equivalent transverse relaxation time can effectively reflect the changes in molecular structure before and after aging, as well as the aging state of the material.

Bi, M. et al. [162] conducted a 100 h corona aging experiment on composite insulators. This experiment was performed at 40%, 60%, 80%, and 95% relative humidities. The samples were subjected to NMR to detect the aging of the samples, and the NMR analysis equipment is shown in Figure 9c [162]. The NMR plots of the same region at different humidity levels were obtained from the test, as shown in Figure 9a,b,d,e [162], and the effective transverse relaxation time $T_{2\text{eff}}$ of the aged samples could be calculated. By comparison, it was found that the decrease of $T_{2\text{eff}}$ was greater with the increase in relative humidity. This indicates that the molecular structure of the silicone rubber material changes more significantly with an increase of the ambient relative humidity. The insulators were also divided into four zones by drawing circles spaced at 10 mm from the center and tested as shown in Figure 9f [162]. It was found that the corona aging was more severe in the central area and less severe in the edge areas.

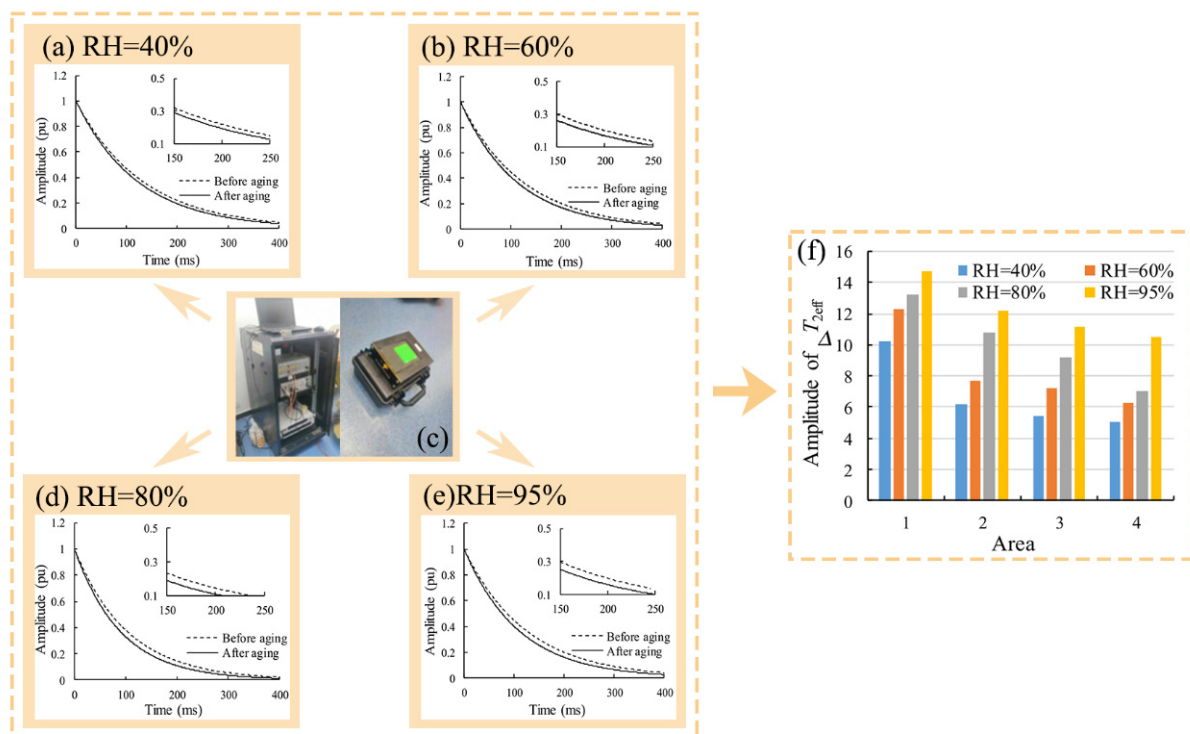


Figure 9. Detection of composite insulators by NMR. (c) NMR detection equipment. (a,b,d,e) NMR curves at different humidity levels. (f) $T_{2\text{eff}}$ values for four different areas and different humidity levels.

Xu, Z. et al. [163] designed a simple and convenient portable NMR sensor. This device can easily detect the sheath layer of curved silicone rubber insulators. It was also used to successfully detect three points on a silicone rubber composite insulator operating for 0, 8,

and 12 years for measurement. He obtained the transverse relaxation decay curves using the CPMG sequence. The relaxation time T_2 was 86 ms, 79 ms and 70 ms by inverse Laplace transform. The relaxation time decreases with increasing aging time. Therefore, the aging of composite insulators can be judged via the method of nuclear magnetic resonance.

5.5. Fourier Transform Infrared Spectroscopy (FTIR)

Fourier infrared spectroscopy is performed by emitting continuous infrared radiation to a sample to obtain the absorption bands of the chemical bonds of the sample. When the infrared radiation of a certain wavelength is exactly equal to the energy required for a certain vibrational or rotational energy level of a group to jump from a ground state to an excited state, the infrared radiation of this wavelength is absorbed by the sample, and the infrared spectrometer can record the formed absorption band. Fourier infrared transform spectroscopy allows analysis of the process of the breaking and forming of chemical bonds within composite insulators. This method is used to understand the aging mechanisms of composite insulators by means of microscopic chemical bonds and to judge the aging degrees of composite insulators.

Zhang, Z. et al. [164] first tested the composite insulators in a salt spray environment for 2 h, 4 h, 6 h, and 8 h with a Fourier infrared spectrometer (ALPHA Fourier infrared spectrometer manufactured by Bruker, Germany), as shown in Figure 10a [164]. It was found that the characteristic peaks of $\text{Si}-(\text{CH}_3)_2$ and $\text{Si}-\text{CH}_3$ decreased with an increase in time. This is because, during the aging process, the side chain is sheared, resulting in the decrease of hydrophobic $-\text{CH}_3$. $-\text{CH}_3$ is closely related to the hydrophobicity of the sample. The absorption peak of $\text{Si}-\text{O}-\text{Si}$ also decreased substantially. This is because the main chain of composite insulator has been broken. The decrease of these peaks increases with the advancement of aging. Zhang, Z. et al. [5] also tested the Fourier infrared spectra (ALPHA Fourier infrared spectrometer manufactured by Bruker, Germany) of different voltages in a salt spray environment, as shown in Figure 10b [5]. They found that the absorption peaks of $\text{Si}-(\text{CH}_3)_2$, $\text{Si}-\text{CH}_3$, and $\text{Si}-\text{O}-\text{Si}$ decreased with an increase in voltage.

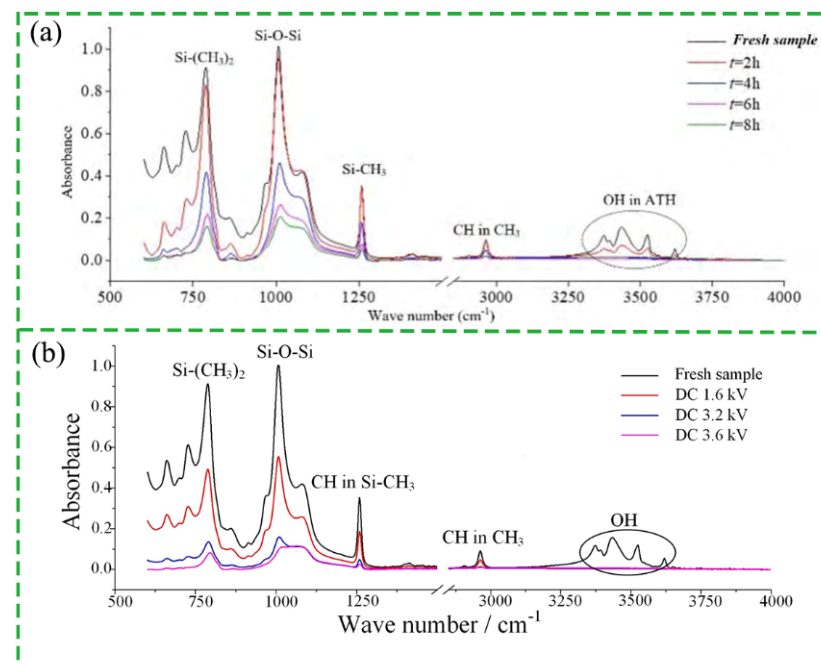


Figure 10. FTIR spectra. (a) FTIR spectra of composite insulators operated for 2 h, 4 h, 6 h and 8 h in a salt fog environment. (b) FTIR spectra of DC 1.6 kV, 3.2 kV and 3.6 kV composite insulators in a salt fog environment.

Rowland, M.S. et al. [165] removed 18 composite insulators that had been in operation for 15 years directly from a 400 kV transmission line in southwest England. The infrared spectroscopy conducted shows that due to the influence of aging, the number of polymer groups corresponding to the Si-CH₃ bond decreases, while the number of groups corresponding to the O-H bond increases, as observed with a Fourier infrared spectrometer (Perkin Elmer Autoimage FTIR microscope system). The concentration of Si-O-Si bonds was generally higher on the bottom exfoliated surface than on the top exfoliated surface. This decrease in chemical bonding suggests chain breakage due to high-energy damage and some form of arcing activity on the top surface. Therefore, it is possible to detect the aging state of the composite insulators by measuring the chemical bond breakage through FTIR spectroscopy.

5.6. The X-ray Photoelectron Spectroscopy (XPS) Method

In 1954, Professor K. Siegbahn, academician of the Royal Swedish Academy of Sciences and director of the Institute of Physics of Uppsala University, developed the world's first X-ray Photoelectron Spectroscopy (XPS) device. Scientists used this instrument to accurately measure the binding energies of electrons in the inner layer of the periodic table of elements. In 1960, scientists discovered that the change of binding energy in the inner layer of atoms can provide information about the molecular structure and valence state of atoms. Since then, XPS has been widely used in different fields of materials research. XPS is used to obtain the XPS spectrum of the sample by radiating X-rays to the surface of the sample, emitting photoelectrons, collected by the detector and processed by computer. This method is a commonly used material analysis method for detecting the elemental composition, empirical formulae, chemical states, and electronic states present in materials [166,167]. During the aging process of composite insulators, there are chemical bond breaks, and thus the aging state of composite insulators can be determined by these changes in chemical bonds.

Chakraborty, R et al. [168] investigated the effect of dry heat exposure on composite insulators by conducting dry-weather aging tests on composite insulators. XPS (SPECS Om GmbH) was used to quantitatively study the changes of the compositions of fresh samples without thermal stress, with thermal stress, and with electrothermal stress. The experimental results show that the percentages of silicon (Si) and carbon (C) in the samples with thermal stress and electrothermal stress are lower than those without thermal stress. However, the oxygen (O) content increased significantly. This indicates that oxidation occurred on the surface of the samples under dry thermal exposure environment, which aged the composite insulators.

Song, W. et al. [48] found that chemical groups mainly exist in the form of -CH₃, -Si-O, etc. for unaged samples by XPS. After being exposed to corona discharge, however, the original groups are gradually oxidized to show strong polar groups (C-O, -C=O, -OH). With an increase in aging time, the group percentage of these strongly polar components increases. After exposure to corona discharge for four days, methyl (-CH₃) was greatly depleted, and decreased from 53.1% to 27.3% (in atomic percentage). The Si-O-Si bond which constitutes the SIR macromolecular chain also breaks on a large scale, from 24.0% to 14.5%. The degradation process of SIR material under the influence of corona discharge is as follows: The methyl group of macromolecular chains is oxidized and cut into small segments, producing a large number of strongly polar groups, leaving the Si-O-Si molecular chain uncovered. With the oxidation and degradation of external environment such as high temperature, chemical pollution, and ultraviolet rays, the hydrophobicity of composite insulators will decrease.

Chen, C. et al. [169] studied the aging of a hollow core composite insulator with liquid rubber as the shell. This composite insulator dissected the aged shed into three parts: the surface layer, the shallow layer (0.4~0.6 mm deep), and the deep layer (1 mm deep). The XPS experiments revealed that the C-element content increased with the decrease of O-element content when sampling from the surface layer to the deep layer. As the degradation

process proceeds, the cross-linking of Si–O chains increases, and organic groups such as Si–C bonds and CH₃ decrease, which leads to the loss of hydrophobicity and the decrease of mechanical properties. This also implies a change in the microstructure of the sample. Therefore, XPS measures the breakage of chemical bonds and detects the aging state of composite insulators.

5.7. The Photothermal Radiation (PTR) Method

For composite insulators, the thermal and absorption characteristics can be determined quantitatively by photothermal radiometry (PTR). This is a non-destructive and non-contact photothermal measurement technique that enables the nondestructive testing of composite insulators. This method is widely used for the thermal characterization and depth profiling of solid materials. The principle of the photothermal radiation method is based on the photothermal effect. Laser excitation of the sample surface generates thermal waves inside the sample, which carry information on the thermal physics and absorption of the sample. PTR provides a new method based on thermal characteristics for evaluating the aging process of silicone rubber composite insulators. It is expected that more information about the thermal properties will be obtained to better understand the aging processes and performance degradations of silicone rubber composite insulators.

There exists a relationship between thermal properties and materials. Jiang et al. [170] first applied the photothermal radiation method to the aging detection of composite insulators. The PTR model was developed with a photothermal radiation apparatus. They performed photothermal radiation tests on the upper and lower surfaces of composite insulators that had never been used, then composite insulators which had operated for 5 years and 10 years. By comparing the thermal and absorption properties (thermal diffusivity, surface absorption, and volumetric absorption coefficient), a relationship between aging and the thermal diffusivity and absorption properties was shown to exist. It was found that the aging process leads to a decrease in diffusivity and an increase in surface and bulk absorption, and that diffusivity and absorption changes are related to the degree of aging. Through these experimental structures, it was demonstrated that the thermal and absorption properties are useful parameters for assessing the level of aging and understanding the aging mechanism of silicone rubber composite insulators.

Jiang, H. et al. [170] only considered the relationship between the thermal properties of the surface and aging. However, the aging of composite insulators is a dynamic process from the surface to the whole, manifesting as a deep distribution of thermal and optical properties. Jiang, H. et al. [171] developed a two-layer PTR theoretical model based on [170]. Considering the complexity of the actual modeling, the model was simplified to a two-layer theoretical model, i.e., the aging layer and the substrate layer of the composite insulator. The thermal and optical absorption properties and the thickness of the aging layer were obtained. The appearance of the aging layer and the significant difference in thermal diffusivity between the surface and the body demonstrate the validity of using thermal diffusivity as a target parameter for assessing the degree of aging. The aging-induced changes in thermal properties were interpreted as disruptions of the tightly packed structure and bond breakage of the polymer matrix. The depth distribution of the effective thermal diffusivity was obtained by polishing the samples layer by layer. Thus, this method is valid and promising for evaluating the aging process of composite insulators in practical applications.

Jiang, H. et al. [172] continued to use self-normalized photothermal radiometry (PTR) to quantitatively characterize the degree of aging of composite insulators used outdoors based on [170,171]. The ratio of the basal thermal diffusivity normalized to the thermal diffusivity of the aging layer is proposed to characterize the degree of aging. This method eliminates the effect of the variation of the initial thermal diffusivity of fresh silicone rubber composite insulators. The experimental results show that the thermal diffusivity decreases and the thickness of the aging layer increases monotonically with increasing service life, consistent with the measurements of hydrophobic grade. The thermal diffusivity and

thickness of the aging layer are expected to serve as numerical indicators for understanding the aging mechanism and estimating the remaining life of silicone rubber composite insulators in field use.

5.8. Modern Intelligent Testing Technology

Traditional methods have low accuracy and poor applicability in insulator identification and fault detection. In order to improve the accuracy of insulator identification and fault detection, a neural network-based test composite insulator testing method has been developed. The method utilizes a computer, which enables fast and accurate aging and fault detection of composite insulators, replacing the traditional manual testing. Zhao, W. et al. [173] proposed an identification and fault detection model. The method improves the fast region convolutional neural network (RCNN) model based on the feature pyramid networks (FPNs). Through the training of the neural network model, the model can better identify insulators and detect fault types. The experimental results show that the accuracy rate of composite insulator aging detection by this method reaches 91.7%. This method realizes the intelligent fault detection of composite insulators and provides a good method for practical engineering application.

Zhang, D. et al. [174] put forward an aging model of composite insulators based on the BP neural network and gave the life prediction of composite insulators. In this paper, composite insulator samples which have been in operation for 0–13 years are used as the research object. It is found that parameters such as hydrophobic grade, contact angle, and surface hardness are significantly related to the running time of composite insulators. These parameters can accurately characterize the aging degree of composite insulators. The life of composite insulators can be accurately predicted by a training BP neural network. It is of great significance to help study the aging of composite insulators, which is convenient in determining the running time of composite insulators.

The aging detection technology of composite insulators has changed from the traditional single detection methods such as hydrophobicity detection, SEM surface topography detection, thermal stimulation current method, nuclear magnetic resonance, Fourier infrared spectroscopy, X-ray photoelectron spectroscopy, and photothermal radiation method, etc., to intelligent fault detection based on digital image processing and intelligent identification algorithm of multi-parameter fusion neural network, which can more accurately detect the aging state of composite insulators and even predict the service life. In the future, it is believed that more and more detection technologies will emerge, and that composite insulator detection technology will develop in the direction of being more convenient and more accurate.

6. Conclusions

Through researching and summarizing the research status of composite insulators at home and abroad, it is found that composite insulators are widely used in power transmission systems due to their light weight, high strength, and good pollution resistance. Among them, the hydrophobicity of composite insulators can effectively prevent the pollution and flashover accidents of insulators, and it has always been one of the directions to which researchers pay most attention. The preparation methods of superhydrophobic surfaces of silicone rubber composite insulators include the laser engraving method, the stencil method, the coating method, the spraying method, and the hybrid method. The preparation technology of superhydrophobic surfaces is cumbersome, the preparation cost is high, and the durability is low, which restricts the development of composite insulators. Therefore, it is very important to develop low-cost and high-durability composite insulator preparation methods for large-scale production

In areas with frequent snowstorms, weather poses a huge challenge to the safe operation of power systems. Traditional active deicing methods, such as hot melting ice and mechanical deicing, are gradually being eliminated due to criticism of the bulky and inefficient equipment involved. The superhydrophobic surfaces not only have the function

of self-cleaning, but also the function of anti-icing. Passive deicing methods represented by anti-icing surfaces have attracted researchers' attention, and more and more methods for preparing superhydrophobic surfaces with anti-icing effects have been developed. However, their hydrophobicity and anti-icing properties are greatly reduced in extreme environments. By adding photothermal, electrothermal, and magnetothermal plasma into the insulator, the conventional superhydrophobic anti-icing surface is endowed with thermal performance, and the perfect combination of active anti-icing and passive anti-icing is achieved. In the future, composite insulators will continue to develop in the direction of increased functionality and stronger performance.

In the long-term outdoor operation process, composite insulators will be affected by ultraviolet rays, fog, algae, bird droppings, low temperature, and other environmental influences, resulting in pulverization and cracking of their surfaces. It is very important for the normal operation of composite insulators to know the aging degree of composite insulators accurately, and to give early warning to the service life of composite insulators. The aging detection technology of composite insulators has developed from the traditional hydrophobicity detection, such as SEM surface morphology detection, the thermal stimulation current method, nuclear magnetic resonance, Fourier infrared spectrum, X-ray photoelectron spectrum, the photothermal radiation method, and so on, towards the intelligent fault detection based on digital image processing and intelligent identification algorithm of multi-parameter fusion neural network, which can accurately detect the aging state of composite insulators and even predict the service life. In the future, it is believed that more and more detection technologies will emerge, and the composite insulator detection technology will develop towards greater convenience and accuracy.

Author Contributions: Conceptualization, Q.H. and W.H.; methodology, F.Z. (Fengwei Zhang) and F.Z. (Fangyuan Zhang); validation, L.L., Y.Z. and X.Y.; formal analysis, Q.H. and F.Z. (Fengwei Zhang); investigation, W.H., F.Z. (Fangyuan Zhang) and Y.Z.; resources, L.L.; data curation, X.Y.; writing—original draft preparation, W.H.; writing—review and editing, Q.H.; visualization, F.Z. (Fengwei Zhang); supervision, Q.H.; project administration, Q.H.; funding acquisition, Q.H. All authors have read and agreed to the published version of the manuscript.

Funding: This research project was supported by the National Modern Agricultural Industry Technology System (CARS-14-1-28).

Institutional Review Board Statement: Not applicable.

Informed Consent Statement: Not applicable.

Data Availability Statement: The data that support the findings of this study are available from the corresponding author, upon reasonable request.

Conflicts of Interest: The authors declare no conflict of interest.

References

1. Akbar, M.; Ullah, R.; Alam, S. Aging of silicone rubber-based composite insulators under multi-stressed conditions: An overview. *Mater. Res. Express* **2019**, *6*, 102003. [[CrossRef](#)]
2. Lu, M. *Insulator Application and Fault Case Analysis*; China Power Press: Beijing, China, 2020.
3. Reddy, B.S.; Prasad, D.S. Effect of coldfog on the corona induced degradation of silicone rubber samples. *IEEE Trans. Dielectr. Electr. Insul.* **2015**, *22*, 1711–1718. [[CrossRef](#)]
4. Reddy, B.S.; Prasad, D.S. Corona degradation of the polymer insulator samples under different fog conditions. *IEEE Trans. Dielectr. Electr. Insul.* **2016**, *23*, 359–367. [[CrossRef](#)]
5. Zhang, Z.; Liang, T.; Li, C.; Jiang, X.; Wu, J.; Wu, B. Electrical strength and physicochemical performances of HTV silicone rubber under salt-fog environment with DC energized. *Polymers* **2020**, *12*, 324. [[CrossRef](#)]
6. Yang, S.; Jia, Z.; Ouyang, X.; Bai, H.; Liu, R. Hydrophobicity characteristics of algae-fouled HVDC insulators in subtropical climates. *Electr. Power Syst. Res.* **2018**, *163*, 626–637. [[CrossRef](#)]
7. Ouyang, X.; Yin, F.; Jia, Z.; Yang, S.; Wang, Y.; Bai, H.; Zhang, X.; Li, Y.; Chen, H. Research of biological contamination and its effect on the properties of RTV-coated insulators. *Electr. Power Syst. Res.* **2019**, *167*, 138–149. [[CrossRef](#)]

8. Ouyang, X.; Jia, Z.; Yang, S.; Shang, X.; Wang, X.; Chen, H.; Zhou, D.; Liu, R. Influence of algae growth on the external insulation performance of HVDC insulators. *IEEE Trans. Dielectr. Electr. Insul.* **2018**, *25*, 263–271. [[CrossRef](#)]
9. Peng, K.; Liu, C.; Zhu, H.; Xu, Y.; Liu, J.; Chen, C. Simulation experimental study on bird droppings flashover characteristics of transmission lines in tropical areas. *High Volt. Technol.* **2016**, *42*, 248–255. (In Chinese) [[CrossRef](#)]
10. Liu, S.; Wu, B.; Wu, X.; Chen, H.; Li, X.; Chang, B.; Jia, Z.; Xu, X.; Ouyang, X.; Li, Y. Study on bird droppings flashover characteristics of composite insulators for 330 kV transmission lines. *High-Volt. Electr. Appar.* **2018**, *54*, 135–141. (In Chinese) [[CrossRef](#)]
11. Savadkoobi, E.M.; Mirzaie, M.; Seyyedbarzegar, S.M.; Mohammadi, M.; Khodsuz, M.; Pashakolae, M.G.; Ghadikolaei, M.B. Experimental investigation on composite insulators AC flashover performance with fan-shaped non-uniform pollution under electro-thermal stress. *Int. J. Electr. Power Energy Syst.* **2020**, *121*, 106142. [[CrossRef](#)]
12. Park, J.-J.; Kim, J.-S.; Yoon, C.-Y.; Shin, S.-S.; Lee, J.-Y.; Cheong, J.-H.; Kim, Y.-W.; Kang, G.-B. Mechanical and Electrical Properties of Cycloaliphatic Epoxy/Silica Systems for Electrical Insulators for Outdoor Applications. *Trans. Electr. Electron. Mater.* **2015**, *16*, 82–85. [[CrossRef](#)]
13. Zhao, M.; Li, W.; Wu, Y.; Zhao, X.; Tan, M.; Xing, J. Performance Investigation on Different Designs of Superhydrophobic Surface Texture for Composite Insulator. *Materials* **2019**, *12*, 1164. [[CrossRef](#)] [[PubMed](#)]
14. Liang, X.; Wang, S.; Fan, J.; Guan, Z. Development of composite insulators in China. *IEEE Trans. Dielectr. Electr. Insul.* **1999**, *6*, 586–594. [[CrossRef](#)]
15. Reddy, B.S.; Ramamurthy, P.C. Analysis of in-service composite insulators used in overhead railway traction. *Eng. Fail. Anal.* **2020**, *108*, 104227. [[CrossRef](#)]
16. Rogelj, J.; Schaeffer, M.; Meinshausen, M.; Knutti, R.; Alcamo, J.; Riahi, K.; Hare, W. Zero emission targets as long-term global goals for climate protection. *Environ. Res. Lett.* **2015**, *10*, 105007. [[CrossRef](#)]
17. Energy Transitions Commission. *China 2050: A Fully Developed Rich Zero-Carbon Economy*; Energy Transitions Commission: Beijing, China, 2019.
18. Li, J.; Hou, M.S.; Xie, C.; Stern, N. China's flexibility challenge in achieving carbon neutrality by 2060. *Renew. Sustain. Energy Rev.* **2022**, *158*, 112112. [[CrossRef](#)]
19. Xie, L.; Singh, C.; Mitter, S.K.; Dahleh, M.A.; Oren, S.S. Toward carbon-neutral electricity and mobility: Is the grid infrastructure ready? *Joule* **2021**, *5*, 1908–1913. [[CrossRef](#)]
20. Ou, Y.; Kittner, N.; Babae, S.; Smith, S.J.; Nolte, C.G.; Loughlin, D.H. Evaluating long-term emission impacts of large-scale electric vehicle deployment in the US using a human-Earth systems model. *Appl. Energy* **2021**, *300*, 117364. [[CrossRef](#)]
21. Li, J.; Sun, C. Towards a low carbon economy by removing fossil fuel subsidies? *China Econ. Rev.* **2018**, *50*, 17–33. [[CrossRef](#)]
22. Li, C.; Yang, Y.; Xu, G.; Zhou, Y.; Jia, M.; Zhong, S.; Gao, Y.; Park, C.; Liu, Q.; Wang, Y.; et al. Insulating materials for realising carbon neutrality: Opportunities, remaining issues and challenges. *High Volt.* **2022**. [[CrossRef](#)]
23. Wang, F.; Huang, H.; He, R.; Pan, X. Composite Insulator's Hydrophobicity Detection Method Based on Sparse Representation Classification Algorithm. *J. Hunan Univ. Nat. Sci.* **2014**, *41*, 98–102.
24. Hillborg, H.; Gedde, U.W. Hydrophobicity changes in silicone rubbers. *IEEE Trans. Dielectr. Electr. Insul.* **1999**, *6*, 703–717. [[CrossRef](#)]
25. Qiao, X.; Zhang, Z.; Jiang, X.; Sundararajan, R.; You, J. DC pollution flashover performance of HVDC composite insulator under different non-uniform pollution conditions. *Electr. Power Syst. Res.* **2020**, *185*, 106351. [[CrossRef](#)]
26. Jiang, X.; Yuan, J.; Zhang, Z.; Hu, J.; Sun, C. Study on AC Artificial-Contaminated Flashover Performance of Various Types of Insulators. *IEEE Trans. Power Deliv.* **2007**, *22*, 2567–2574. [[CrossRef](#)]
27. Jiang, X.; Yuan, J.; Zhang, Z.; Hu, Q.; Cheng, A. Study on AC pollution flashover performance of composite insulators at high altitude sites of 2800–4500 m. *IEEE Trans. Dielectr. Electr. Insul.* **2009**, *16*, 123–132. [[CrossRef](#)]
28. Wang, J.; Zhang, Y.; Ding, J.; Xu, Z.; Zhang, J.; He, Q. Preparation strategy and evaluation method of durable superhydrophobic rubber composites. *Adv. Colloid Interface Sci.* **2021**, *299*, 102549. [[CrossRef](#)] [[PubMed](#)]
29. Zhou, W.; Ma, Y.; He, Q. Investigation of self-cleaning and bouncing properties of superhydrophobic alu-minum nitride/silicone rubber. *J. Appl. Polym. Sci.* **2022**, *139*, 51990. [[CrossRef](#)]
30. He, Q.; Xu, Z.; Li, A.; Wang, J.; Zhang, J.; Zhang, Y. Study on hydrophobic properties of fluororubber prepared by template method under high temperature conditions. *Colloids Surf. A Physicochem. Eng. Asp.* **2020**, *612*, 125837. [[CrossRef](#)]
31. Patil, D.; Aravindan, S.; Sarathi, R.; Rao, P.V. Fabrication of self-cleaning superhydrophobic silicone rubber insulator through laser texturing. *Surf. Eng.* **2020**, *37*, 308–317. [[CrossRef](#)]
32. Jin, H.; Jin, P.; Niu, R.; Li, Y.; He, B.; Gao, N.; Zhang, H. Flashover characteristics of discrete water droplets on the surface of super-hydrophobic silicone rubber. *IEEE Trans. Dielectr. Electr. Insul.* **2014**, *21*, 1718–1725. [[CrossRef](#)]
33. Wang, G.; Zhou, J.; Wang, M.; Zhang, Y.; Zhang, Y.; He, Q. A superhydrophobic surface with aging resistance, excellent mechanical restorability and droplet bounce properties. *Soft Matter* **2020**, *16*, 5514–5524. [[CrossRef](#)] [[PubMed](#)]
34. Li, J.; Zhao, Y.; Hu, J.; Shu, L.; Shi, X. Anti-icing Performance of a Superhydrophobic PDMS/Modified Nano-silica Hybrid Coating for Insulators. *J. Adhes. Sci. Technol.* **2012**, *26*, 665–679. [[CrossRef](#)]

35. Peng, W.; Gou, X.; Qin, H.; Zhao, M.; Zhao, X.; Guo, Z. Robust Mg(OH)₂/epoxy resin superhydrophobic coating applied to composite insulators. *Appl. Surf. Sci.* **2019**, *466*, 126–132. [[CrossRef](#)]
36. Li, Y.; Jin, H.; Nie, S.; Zhang, P.; Gao, N. Dynamic behavior of water droplets and flashover characteristics on a superhydrophobic silicone rubber surface. *Appl. Phys. Lett.* **2017**, *110*, 201602. [[CrossRef](#)]
37. Lei, S.; Wang, F.; Fang, X.; Ou, J.; Li, W. Icing behavior of water droplets impinging on cold superhydrophobic surface. *Surf. Coat. Technol.* **2019**, *363*, 362–368. [[CrossRef](#)]
38. Vallabhuneni, S.; Movafaghi, S.; Wang, W.; Kota, A.K. Superhydrophobic Coatings for Improved Performance of Electrical Insulators. *Macromol. Mater. Eng.* **2018**, *303*, 1800313. [[CrossRef](#)]
39. Yan, Z.; Liang, X.; Cotton, I.; Emersic, C. Suppression of surface charge on micro- and nano-structured superhydrophobic silicone rubber. *IEEE Trans. Dielectr. Electr. Insul.* **2018**, *25*, 1095–1102. [[CrossRef](#)]
40. Zhang, H.; Yang, Y.; Pan, J.; Long, H.; Huang, L.; Zhang, X. Compare study between icephobicity and superhydrophobicity. *Phys. B Condens. Matter* **2019**, *556*, 118–130. [[CrossRef](#)]
41. Arianpour, F.; Farzaneh, M. On Hydrophobic and Icephobic Properties of TiO₂-Doped Silicon Rubber Coatings. *Int. J. Theor. Appl. Nanotechnol.* **2012**, *1*, 79–85. [[CrossRef](#)]
42. De Pauw, D.; Dolatabadi, A. Effect of Superhydrophobic Coating on the Anti-Icing and Deicing of an Airfoil. *J. Aircr.* **2017**, *54*, 490–499. [[CrossRef](#)]
43. Liu, B.; Zhang, K.; Tao, C.; Zhao, Y.; Li, X.; Zhu, K.; Yuan, X. Strategies for anti-icing: Low surface energy or liquid-infused? *RSC Adv.* **2016**, *6*, 70251–70260. [[CrossRef](#)]
44. Chen, C.; Tian, Z.; Luo, X.; Jiang, G.; Hu, X.; Wang, L.; Peng, R.; Zhang, H.; Zhong, M. Micro–Nano–Nanowire Triple Structure-Held PDMS Superhydrophobic Surfaces for Robust Ultra-Long-Term Icephobic Performance. *ACS Appl. Mater. Interfaces* **2022**, *14*, 23973–23982. [[CrossRef](#)] [[PubMed](#)]
45. Mehmood, B.; Akbar, M.; Ullah, R. Accelerated aging effect on high temperature vulcanized silicone rubber composites under DC voltage with controlled environmental conditions. *Eng. Fail. Anal.* **2020**, *118*, 104870.
46. Jing, P.; Zhiqiang, L.; Peng, W.; Qian, J.; Chunjie, W.; Yuxin, L. Research on Ultraviolet Aging Properties of Modified Silicone Rubber for Composite Insulator. In Proceedings of the 2020 International Symposium on Electrical Insulating Materials (ISEIM), Tokyo, Japan, 13–17 September 2020.
47. Wakhidin, M. Effects of artificial tropical climate aging on insulation performance of silicone rubber polymeric insulators. In Proceedings of the 2019 2nd International Conference on High Voltage Engineering and Power Systems (ICHVEPS), Denpasar, Indonesia, 1–4 October 2019.
48. Song, W.; Shen, W.W.; Zhang, G.J.; Song, B.P.; Lang, Y.; Su, G.Q.; Deng, J.B. Aging characterization of high temperature vulcanized silicone rubber housing material used for outdoor insulation. *IEEE Trans. Dielectr. Electr. Insul.* **2015**, *22*, 961–969. [[CrossRef](#)]
49. Israrullah; Amin, M.; Mahmood, A.; Khattak, A. Accelerated multi stress aging and life estimation of polymeric insulators. In Proceedings of the 2020 17th International Bhurban Conference on Applied Sciences and Technology (IBCAST), Islamabad, Pakistan, 14–18 January 2020.
50. Dong, B.; Zhang, Z.; Xiang, N.; Yang, H.; Xu, S.; Cheng, T. AC Flashover Voltage Model for Polluted Suspension Insulators and an Experimental Investigation in Salt Fog. *IEEE Access* **2020**, *8*, 187411–187418. [[CrossRef](#)]
51. Liu, Y.; Zong, H.; Gao, S.; Du, B.X. Contamination deposition and discharge characteristics of outdoor insulators in fog-haze conditions. *Int. J. Electr. Power Energy Syst.* **2020**, *121*, 106176. [[CrossRef](#)]
52. Salem, A.A.; Rahman, R.A.; Al-Ameri, S. Pollution Flashover Characteristics of High-Voltage Outdoor Insulators: Analytical Study. *Arab. J. Sci. Eng.* **2022**, *47*, 2711–2729. [[CrossRef](#)]
53. Salem, A.A.; Abd-Rahman, R.; Rahiman, W.; Al-Gailani, S.A.; Al-Ameri, S.M.; Ishak, M.T.; Sheikh, U.U. Pollution Flashover Under Different Contamination Profiles on High Voltage Insulator: Numerical and Experiment Investigation. *IEEE Access* **2021**, *9*, 37800–37812. [[CrossRef](#)]
54. Farzaneh, M.; Chisholm, W.A. 50 years in icing performance of outdoor insulators. *IEEE Electr. Insul. Mag.* **2014**, *30*, 14–24. [[CrossRef](#)]
55. Olad, A.; Maryami, F.; Mirmohseni, A.; Shayegani-Akmal, A.A. Potential of slippery liquid infused porous surface coatings as flashover inhibitors on porcelain insulators in icing, contaminated, and harsh environments. *Prog. Org. Coat.* **2021**, *151*, 106082. [[CrossRef](#)]
56. Li, A.; Wang, J.; Ren, S.; Zhang, J.; Zhang, X.; Zhang, Y. Preparation of superhydrophobic paper mulch and study on its anti-UV performance. *J. Saudi Chem. Soc.* **2021**, *25*, 101322. [[CrossRef](#)]
57. Li, A.; Wang, G.; Ma, Y.; Zhao, C.; Zhang, F.; He, Q.; Zhang, F. Study on preparation and properties of superhydrophobic surface of RTV silicone rubber. *J. Mater. Res. Technol.* **2021**, *11*, 135–143. [[CrossRef](#)]
58. Ma, Y.; He, Q. Preparation of superhydrophobic conductive CNT/PDMS film on paper by foam spraying method. *Colloids Surf. A Physicochem. Eng. Asp.* **2022**, *648*, 129327. [[CrossRef](#)]
59. Millionis, A.; Loth, E.; Bayer, I.S. Recent advances in the mechanical durability of superhydrophobic materials. *Adv. Colloid Interface Sci.* **2016**, *229*, 57–79. [[CrossRef](#)]

60. Fihri, A.; Bovero, E.; Al-Shahrani, A.; Al-Ghamdi, A.; Alabedi, G. Recent progress in superhydrophobic coatings used for steel protection: A review. *Colloids Surf. A Physicochem. Eng. Asp.* **2017**, *520*, 378–390. [[CrossRef](#)]
61. Qi, Y.; Cui, Z.; Liang, B.; Parnas, R.S.; Lu, H. A fast method to fabricate superhydrophobic surfaces on zinc substrate with ion assisted chemical etching. *Appl. Surf. Sci.* **2014**, *305*, 716–724. [[CrossRef](#)]
62. Peng, S.; Yang, X.; Tian, D.; Deng, W. Chemically Stable and Mechanically Durable Superamphiphobic Aluminum Surface with a Micro/Nanoscale Binary Structure. *ACS Appl. Mater. Interfaces* **2014**, *6*, 15188–15197. [[CrossRef](#)]
63. Liu, X.; Xu, Y.; Ben, K.; Chen, Z.; Wang, Y.; Guan, Z. Transparent, durable and thermally stable PDMS-derived superhydrophobic surfaces. *Appl. Surf. Sci.* **2015**, *339*, 94–101.
64. Chen, X.; Hong, L.; Xu, Y.; Ong, Z.W. Ceramic Pore Channels with Inducted Carbon Nanotubes for Removing Oil from Water. *ACS Appl. Mater. Interfaces* **2012**, *4*, 1909–1918. [[CrossRef](#)]
65. Milionis, A.; Languasco, J.; Loth, E.; Bayer, I.S. Analysis of wear abrasion resistance of superhydrophobic acrylonitrile butadiene styrene rubber (ABS) nanocomposites. *Chem. Eng. J.* **2015**, *281*, 730–738. [[CrossRef](#)]
66. Mendoza, A.I.; Moriana, R.; Hillborg, H.; Strömberg, E. Super-hydrophobic zinc oxide/silicone rubber nanocomposite surfaces. *Surf. Interfaces* **2019**, *14*, 146–157. [[CrossRef](#)]
67. Li, L.; Huang, T.; Lei, J.; He, J.; Qu, L.; Huang, P.; Zhou, W.; Li, N.; Pan, F. Robust biomimetic-structural superhydrophobic surface on aluminum alloy. *ACS Appl. Mater. Interfaces* **2015**, *7*, 1449–1457. [[CrossRef](#)] [[PubMed](#)]
68. Zhou, H.; Wang, H.; Niu, H.; Gestos, A.; Wang, X.; Lin, T. Fluoroalkyl Silane Modified Silicone Rubber/Nanoparticle Composite: A Super Durable, Robust Superhydrophobic Fabric Coating. *Adv. Mater.* **2012**, *24*, 2409–2412. [[CrossRef](#)] [[PubMed](#)]
69. Kong, L.-H.; Chen, X.-H.; Yu, L.-G.; Wu, Z.-S.; Zhang, P.-Y. Superhydrophobic cuprous oxide nanostructures on phosphor-copper meshes and their oil-water separation and oil spill cleanup. *ACS Appl. Mater. Interfaces* **2015**, *7*, 2616–2625. [[CrossRef](#)]
70. Leventis, N.; Chidambareswarapattar, C.; Bang, A.; Sotiriou-Leventis, C. Cocoon-in-Web-Like Superhydrophobic Aerogels from Hydrophilic Polyurea and Use in Environmental Remediation. *ACS Appl. Mater. Interfaces* **2014**, *6*, 6872–6882. [[CrossRef](#)]
71. Jaafar, H.T.; Aldabbagh, B.M.D. Investigation of superhydrophobic/hydrophobic materials properties using electrospinning technique. *Baghdad Sci. J.* **2019**, *16*, 632–638.
72. Lee, S.; Kim, B.; Kim, S.-H.; Kim, E.; Jang, J.-H. Superhydrophobic, Reversibly Elastic, Moldable, and Electrospun (SupREME) Fibers with Multimodal Functions: From Oil Absorbents to Local Drug Delivery Adjuvants. *Adv. Funct. Mater.* **2017**, *27*, 1702310. [[CrossRef](#)]
73. Huang, Y.; Sarkar, D.; Chen, X.-G. Superhydrophobic nanostructured ZnO thin films on aluminum alloy substrates by electrophoretic deposition process. *Appl. Surf. Sci.* **2015**, *327*, 327–334. [[CrossRef](#)]
74. Xu, L.; Tong, F.; Lu, X.; Lu, K.; Lu, Q. Multifunctional polypyrene/silica hybrid coatings with stable excimer fluorescence and robust superhydrophobicity derived from electrodeposited polypyrene films. *J. Mater. Chem. C* **2015**, *3*, 2086–2092. [[CrossRef](#)]
75. Liu, J.; Xiao, X.; Shi, Y.; Wan, C. Fabrication of a superhydrophobic surface from porous polymer using phase separation. *Appl. Surf. Sci.* **2014**, *297*, 33–39. [[CrossRef](#)]
76. Amin, M.; Akbar, M.; Salman, M. Composite insulators and their aging: An overview. *Sci. China Technol. Sci.* **2007**, *50*, 697–713. [[CrossRef](#)]
77. Yang, Z.; Jiang, X.; Huang, Y.; Hu, J.; Han, X. Influence of electric field on the ice-coating process of insulators with a different dielectric surface. *IET Sci. Meas. Technol.* **2020**, *14*, 585–592. [[CrossRef](#)]
78. Ramalla, I.; Gupta, R.K.; Bansal, K. Effect on superhydrophobic surfaces on electrical porcelain insulator, improved technique at polluted areas for longer life and reliability. *Int. J. Eng. Technol.* **2015**, *4*, 509. [[CrossRef](#)]
79. Kietzig, A.-M.; Hatzikiriakos, S.G.; Englezos, P. Patterned superhydrophobic metallic surfaces. *Langmuir* **2009**, *25*, 4821–4827. [[CrossRef](#)] [[PubMed](#)]
80. Ta, D.V.; Dunn, A.; Wasley, T.J.; Kay, R.W.; Stringer, J.; Smith, P.J.; Connaughton, C.; Shephard, J.D. Nanosecond laser textured superhydrophobic metallic surfaces and their chemical sensing applications. *Appl. Surf. Sci.* **2015**, *357*, 248–254. [[CrossRef](#)]
81. Wu, B.; Zhou, M.; Li, J.; Ye, X.; Li, G.; Cai, L. Superhydrophobic surfaces fabricated by microstructuring of stainless steel using a femtosecond laser. *Appl. Surf. Sci.* **2009**, *256*, 61–66. [[CrossRef](#)]
82. Yan, Z.; Liang, X.; Shen, H.; Liu, Y. Preparation and basic properties of superhydrophobic silicone rubber with micro-nano hierarchical structures formed by picosecond laser-ablated template. *IEEE Trans. Dielectr. Electr. Insul.* **2017**, *24*, 1743–1750. [[CrossRef](#)]
83. Du, B.; Li, Z. Hydrophobicity, surface charge and DC flashover characteristics of direct-fluorinated RTV silicone rubber. *IEEE Trans. Dielectr. Electr. Insul.* **2015**, *22*, 934–940. [[CrossRef](#)]
84. Maghsoudi, K.; Jafari, R.; Momen, G.; Farzaneh, M. Micro-nanostructured polymer surfaces using injection molding: A review. *Mater. Today Commun.* **2017**, *13*, 126–143. [[CrossRef](#)]
85. Spathi, C.; Young, N.; Heng, J.Y.Y.; Vandeperre, L.J.M.; Cheeseman, C.R. A simple method for preparing super-hydrophobic powder from paper sludge ash. *Mater. Lett.* **2015**, *142*, 80–83. [[CrossRef](#)]
86. Nayak, B.K.; Gupta, M.C. Self-organized micro/nano structures in metal surfaces by ultrafast laser irradiation. *Opt. Lasers Eng.* **2010**, *48*, 940–949. [[CrossRef](#)]

87. Jagdheesh, R.; García-Ballesteros, J.; Ocaña, J. One-step fabrication of near super-hydrophobic aluminum surface by nano-second laser ablation. *Appl. Surf. Sci.* **2016**, *374*, 2–11. [[CrossRef](#)]
88. Wang, X.; Xu, S.; Cong, M.; Li, H.; Gu, Y.; Xu, W. Hierarchical structural nanopore arrays fabricated by pre-patterning aluminum using nanosphere lithography. *Small* **2012**, *8*, 972–976. [[CrossRef](#)]
89. Ali, H.M.; Qasim, M.A.; Malik, S.; Murtaza, G. Techniques for the fabrication of super-hydrophobic surfaces and their heat transfer applications. *Heat Transf. Models Methods Appl.* **2018**, *1*, 283–315.
90. Kim, H.-M.; Choi, J.-W.; Kwon, J.-S.; Lee, C.-H.; Kim, B. Super-Hydrophobic Properties of Aluminum Surfaces Synthesized by a Two-Step Chemical Etching Process. *J. Nanosci. Nanotechnol.* **2019**, *19*, 6452–6457. [[CrossRef](#)]
91. Liu, Y.; Liu, J.; Li, S.; Wang, Y.; Han, Z.; Ren, L. One-step method for fabrication of biomimetic superhydrophobic surface on aluminum alloy. *Colloids Surf. A Physicochem. Eng. Asp.* **2015**, *466*, 125–131. [[CrossRef](#)]
92. Zheng, S.; Li, C.; Fu, Q.; Hu, W.; Xiang, T.; Wang, Q.; Du, M.; Liu, X.; Chen, Z. Development of stable superhydrophobic coatings on aluminum surface for corrosion-resistant, self-cleaning, and anti-icing applications. *Mater. Des.* **2016**, *93*, 261–270. [[CrossRef](#)]
93. Zhang, Y.; Yu, X.; Wu, H.; Wu, J. Facile fabrication of superhydrophobic nano-structures on aluminum foils with controlled-condensation and delayed-icing effects. *Appl. Surf. Sci.* **2012**, *258*, 8253–8257. [[CrossRef](#)]
94. Christiansen, A.B.; Clausen, J.S.; Mortensen, N.A.; Kristensen, A. Injection moulding antireflective nanostructures. *Microelectron. Eng.* **2014**, *121*, 47–50. [[CrossRef](#)]
95. Holthusen, A.-K.; Riemer, O.; Schmütz, J.; Meier, A. Mold machining and injection molding of diffractive microstructures. *J. Manuf. Process.* **2017**, *26*, 290–294. [[CrossRef](#)]
96. Nagato, K.; Hamaguchi, T.; Nakao, M. Injection compression molding of high-aspect-ratio nanostructures. *J. Vac. Sci. Technol. B Nanotechnol. Microelectron. Mater. Process. Meas. Phenom.* **2011**, *29*, 06FG10. [[CrossRef](#)]
97. Masato, D.; Sorgato, M.; Lucchetta, G. Characterization of the micro injection-compression molding process for the replication of high aspect ratio micro-structured surfaces. *Microsyst. Technol.* **2017**, *23*, 3661–3670. [[CrossRef](#)]
98. Chen, Y.; Yi, A.Y.; Yao, D.; Klocke, F.; Pongs, G. A reflow process for glass microlens array fabrication by use of precision compression molding. *J. Micromech. Microeng.* **2008**, *18*, 055022. [[CrossRef](#)]
99. Chun, D.-M.; Davaasuren, G.; Ngo, C.-V.; Kim, C.-S.; Lee, G.-Y.; Ahn, S.-H. Fabrication of transparent superhydrophobic surface on thermoplastic polymer using laser beam machining and compression molding for mass production. *CIRP Ann. Manuf. Technol.* **2014**, *63*, 525–528. [[CrossRef](#)]
100. He, P.; Li, L.; Wang, F.; Dambon, O.; Klocke, F.; Flores, K.; Yi, A.Y. Bulk metallic glass mold for high volume fabrication of micro optics. *Microsyst. Technol.* **2016**, *22*, 617–623. [[CrossRef](#)]
101. Peng, L.; Deng, Y.; Yi, P.; Lai, X. Micro hot embossing of thermoplastic polymers: A review. *J. Micromech. Microeng.* **2013**, *24*, 013001. [[CrossRef](#)]
102. Wang, J.; Yi, P.; Deng, Y.; Peng, L.; Lai, X.; Ni, J. Recovery behavior of thermoplastic polymers in micro hot embossing process. *J. Mater. Process. Technol.* **2017**, *243*, 205–216. [[CrossRef](#)]
103. Liu, X.; Wu, W.; Wang, X.; Luo, Z.; Liang, Y.; Zhou, F. A replication strategy for complex micro/nanostructures with superhydrophobicity and superoleophobicity and high contrast adhesion. *Soft Matter* **2009**, *5*, 3097–3105. [[CrossRef](#)]
104. Zylka, P. On the surface performance of superhydrophobic silicone rubber specimens fabricated by direct replica method. *IEEE Trans. Dielectr. Electr. Insul.* **2014**, *21*, 1183–1188. [[CrossRef](#)]
105. Seyedmehdi, S.; Zhang, H.; Zhu, J. Influence of production method, silicone type and thickness on silicon rubber superhydrophobic coatings. *Prog. Org. Coat.* **2016**, *90*, 291–295. [[CrossRef](#)]
106. Allahdini, A.; Momen, G.; Munger, F.; Brettschneider, S.; Fofana, I.; Jafari, R. Performance of a nanotextured superhydrophobic coating developed for high-voltage outdoor porcelain insulators. *Colloids Surf. A Physicochem. Eng. Asp.* **2022**, *649*, 129461. [[CrossRef](#)]
107. Ribeiro, A.C.; Soares, B.G.; Furtado, J.G.M.; Silva, A.A.; Couto, N.S.S.E. Superhydrophobic nanocomposite coatings based on different polysiloxane matrices designed for electrical insulators. *Prog. Org. Coat.* **2022**, *168*, 106867. [[CrossRef](#)]
108. Caldon, E.B.; De Leon, A.C.C.; Thomas, P.G.; Naylor, D.F., III; Pajarito, B.B.; Advincula, R.C. Superhydrophobic rubber-modified polybenzoxazine/SiO₂ nanocomposite coating with anti-corrosion, anti-ice, and superoleophilicity properties. *Ind. Eng. Chem. Res.* **2017**, *56*, 1485–1497. [[CrossRef](#)]
109. Pashinin, A.S.; Emel'Yanenko, A.M.; Boinovich, L.B. Interaction between hydrophobic and superhydrophobic materials with aqueous media. *Prot. Met. Phys. Chem. Surf.* **2010**, *46*, 734–739. [[CrossRef](#)]
110. Boinovich, L.B.; Domantovskiy, A.G.; Emelyanenko, A.M.; Pashinin, A.S.; Ionin, A.A.; Kudryashov, S.I.; Saltuganov, P.N. Femtosecond Laser Treatment for the Design of Electro-insulating Superhydrophobic Coatings with Enhanced Wear Resistance on Glass. *ACS Appl. Mater. Interfaces* **2014**, *6*, 2080–2085. [[CrossRef](#)] [[PubMed](#)]
111. Emelyanenko, A.M.; Boinovich, L.B.; Bezdomnikov, A.A.; Chulkova, E.V.; Emelyanenko, K.A. Reinforced Superhydrophobic Coating on Silicone Rubber for Longstanding Anti-Icing Performance in Severe Conditions. *ACS Appl. Mater. Interfaces* **2017**, *9*, 24210–24219. [[CrossRef](#)]
112. Zhang, Y.; Zhang, Z.; Jiang, X.; Liang, T.; Zhang, D. Research on Lifespan Prediction of Composite Insulators in a High Altitude Area Experimental Station. *Appl. Sci.* **2019**, *9*, 3364. [[CrossRef](#)]

113. Jiang, X.; Hui, Y. *Transmission Line Icing and Protection*; China Electric Power Press: Beijing, China, 2002. (In Chinese)
114. Farzaneh, M.; Melo, O. Properties and effect of freezing rain and winter fog on outline insulators. *Cold Reg. Sci. Technol.* **1990**, *19*, 33–46. [[CrossRef](#)]
115. Xu, Z.; Jia, Z.; Li, Z.; Wei, X.; Guan, Z.; MacAlpine, M.; Zhao, Y.; Li, Y. Anti-icing performance of RTV coatings on porcelain insulators by controlling the leakage current. *IEEE Trans. Dielectr. Electr. Insul.* **2011**, *18*, 760–766. [[CrossRef](#)]
116. Wang, X.; Hu, J.; Wu, B.; Du, L.; Sun, C. Study on edge extraction methods for image-based icing on-line monitoring on overhead transmission lines. In Proceedings of the International Conference on High Voltage Engineering and Application (ICHVE '08), Chongqing, China, 9–12 November 2008; pp. 661–665.
117. Xu, J.; Yin, F.; Li, L.; Wen, Q.; Wang, H.; Liu, S.; Jia, Z.; Farzaneh, M. Wet Snow Flashover Characteristics of 500-kV AC Insulator Strings with Different Arrangements. *Appl. Sci.* **2019**, *9*, 930. [[CrossRef](#)]
118. Zhao, J.; Guo, R.; Cao, L.; Zhang, F. Improvement of LineROVER: A mobile robot for de-icing of transmission lines. In Proceedings of the 2010 1st International Conference on Applied Robotics for the Power Industry, Montreal, QC, Canada, 5–7 October 2010. [[CrossRef](#)]
119. Yang, Y.; Wang, Y.; Yuan, X.; Chen, Y.; Tan, L. Neural network-based self-learning control for power transmission line deicing robot. *Neural Comput. Appl.* **2013**, *22*, 969–986. [[CrossRef](#)]
120. Corsi, S.R.; Geis, S.W.; Loyo-Rosales, J.E.; Rice, C.P.; Sheesley, R.J.; Failey, A.G.G.; Cancellia, D.A. Characterization of Aircraft Deicer and Anti-Icer Components and Toxicity in Airport Snowbanks and Snowmelt Runoff. *Environ. Sci. Technol.* **2006**, *40*, 3195–3202. [[CrossRef](#)] [[PubMed](#)]
121. Amrhein, C.; Strong, J.E.; Mosher, P.A. Effect of deicing salts on metal and organic matter mobilization in roadside soils. *Environ. Sci. Technol.* **1992**, *26*, 703–709. [[CrossRef](#)]
122. Balordi, M.; Cammi, A.; de Magistris, G.S.; Chemelli, C. Role of micrometric roughness on anti-ice properties and durability of hierarchical super-hydrophobic aluminum surfaces. *Surf. Coat. Technol.* **2019**, *374*, 549–556. [[CrossRef](#)]
123. Zhao, Z.; Chen, H.; Liu, X.; Liu, H.; Zhang, D. Development of high-efficient synthetic electric heating coating for anti-icing/de-icing. *Surf. Coat. Technol.* **2018**, *349*, 340–346. [[CrossRef](#)]
124. Mobarakeh, L.F.; Jafari, R.; Farzaneh, M. The ice repellency of plasma polymerized hexamethyldisiloxane coating. *Appl. Surf. Sci.* **2013**, *284*, 459–463. [[CrossRef](#)]
125. Peng, W.; Gou, X.; Qin, H.; Zhao, M.; Zhao, X.; Guo, Z. Creation of a multifunctional superhydrophobic coating for composite insulators. *Chem. Eng. J.* **2018**, *352*, 774–781. [[CrossRef](#)]
126. Sun, J.; He, D.; Li, Q.; Zhang, H.; Liu, H. Wettability behavior and anti-icing property of superhydrophobic coating on HTV silicone rubber. *AIP Adv.* **2020**, *10*, 125102. [[CrossRef](#)]
127. Redondo, O.; Prolongo, S.; Campo, M.; Sbarufatti, C.; Giglio, M. Anti-icing and de-icing coatings based Joule's heating of graphene nanoplatelets. *Compos. Sci. Technol.* **2018**, *164*, 65–73. [[CrossRef](#)]
128. Chao, Y.; Wang, F.J.; Li, W.; Ou, J.F.; Li, C.Q.; Amirfazli, A. Anti-icing Properties of Superhydrophobic ZnO/PDMS Composite Coating. *Appl. Phys. A* **2016**, *122*, 1–10.
129. Gam-Derouich, S.; Pinson, J.; Decorse, P.; Luo, Y.; Herbaut, R.; Royon, L.; Mangeney, C. Diazonium salt chemistry for the design of nano-textured anti-icing surfaces. *Chem. Commun.* **2018**, *54*, 8983–8986. [[CrossRef](#)] [[PubMed](#)]
130. Sharifi, N.; Dolatabadi, A.; Pugh, M.; Moreau, C. Anti-icing performance and durability of suspension plasma sprayed TiO₂ coatings. *Cold Reg. Sci. Technol.* **2018**, *159*, 1–12. [[CrossRef](#)]
131. Morita, K.; Sakaue, H. Characterization method of hydrophobic anti-icing coatings. *Rev. Sci. Instrum.* **2015**, *86*, 115108. [[CrossRef](#)]
132. Janjua, Z.A.; Turnbull, B.; Choy, K.L.; Pandis, C.; Liu, J.; Hou, X.; Choi, K.-S. Performance and Durability Tests of Smart Icephobic Coatings to Reduce Ice Adhesion. *Appl. Surf. Sci.* **2017**, *407*, 555–564. [[CrossRef](#)]
133. Guo, J.; Yang, F.; Guo, Z. Fabrication of stable and durable superhydrophobic surface on copper substrates for oil–water separation and ice-over delay. *J. Colloid Interface Sci.* **2016**, *466*, 36–43. [[CrossRef](#)] [[PubMed](#)]
134. Zhao, M.; Yin, Y.; He, Q.; Zhao, X. Anti-icing capability of textured silicone rubber surfaces via laser processing. *Mater. Manuf. Process.* **2021**, *36*, 979–986. [[CrossRef](#)]
135. Hu, J.; Jiang, G. Superhydrophobic coatings on iodine doped substrate with photothermal deicing and passive anti-icing properties. *Surf. Coat. Technol.* **2020**, *402*, 126342. [[CrossRef](#)]
136. Wang, T.; Zheng, Y.; Raji, A.-R.O.; Li, Y.; Sikkema, W.K.A.; Tour, J.M. Passive Anti-Icing and Active Deicing Films. *ACS Appl. Mater. Interfaces* **2016**, *8*, 14169–14173. [[CrossRef](#)]
137. Yin, X.; Zhang, Y.; Wang, D.; Liu, Z.; Liu, Y.; Pei, X.; Yu, B.; Zhou, F. Integration of Self-Lubrication and Near-Infrared Photothermogenesis for Excellent Anti-Icing/Deicing Performance. *Adv. Funct. Mater.* **2015**, *25*, 4237–4245. [[CrossRef](#)]
138. Liao, W.; Jia, Z.; Guan, Z.; Wang, L.; Yang, J.; Fan, J.; Su, Z.; Zhou, J. Reducing Ice Accumulation on Insulators by Applying Semiconducting RTV Silicone Coating. *IEEE Trans. Dielectr. Electr. Insul.* **2007**, *14*, 1446–1454. [[CrossRef](#)]
139. Jiang, G.; Chen, L.; Zhang, S.; Huang, H.-X. Superhydrophobic SiC/CNTs Coatings with Photothermal Deicing and Passive Anti-Icing Properties. *ACS Appl. Mater. Interfaces* **2018**, *10*, 36505–36511. [[CrossRef](#)] [[PubMed](#)]
140. Gubanski, S.; Vlastos, A. Wettability of naturally aged silicon and EPDM composite insulators. *IEEE Trans. Power Deliv.* **1990**, *5*, 1527–1535. [[CrossRef](#)]

141. Wang, Q.-D.; Wen, B.-Y.; Wang, X.-P. Measuring insulating material hydrophobic level by image recognition and classification. *Electr. Mach. Control* **2008**, *12*, 94–98.
142. Fochi, W.; Kang, Y.; Zhongyuan, Z.; Yanbo, W.; Shengjie, Y. Identifying insulator hydrophobicity by image analysis and neural network. *Electr. Mach. Control* **2014**, *18*, 78–83.
143. Pen, K.-X.; Wang, Q.-D.; Wang, X.-P. Spray image analysis based measurement of hydrophobic of insulator surfaces. *Insul. Mater.* **2005**, *7*, 47–51.
144. Yang, S.; Jia, Z.; Ouyang, X. Effects of algae contamination on the hydrophobicity of high-voltage composite insulators. *High Volt.* **2019**, *4*, 234–240. [[CrossRef](#)]
145. Mir, H.; Berkowitz, Z. Sub-band STAP for stretch processed systems. In Proceedings of the 2009 IEEE International Conference on Acoustics, Speech and Signal Processing, Taipei, Taiwan, 19–24 April 2009; pp. 2025–2028. [[CrossRef](#)]
146. Berg, M.; Thottappillil, R.; Scuka, V. A digital image processing method for estimating the level of hydrophobicity of high voltage polymeric insulating materials. In Proceedings of the 1999 Annual Report Conference on Electrical Insulation and Dielectric Phenomena, Austin, TX, USA, 17–20 October 1999; pp. 756–762. [[CrossRef](#)]
147. Li, Z.; Liang, X.; Zhou, Y.; Tang, J.; Cui, J.; Liu, Y. Influence of temperature on the hydrophobicity of silicone rubber surfaces. In Proceedings of the 17th Annu. Meeting IEEE Lasers Electro-Optics Society, Boulder, CO, USA, 20 October 2004; pp. 679–682.
148. Sorqvist, T.; Vlastos, A.E. Performance and ageing of polymeric insulators. *IEEE Trans. Power Deliv.* **1997**, *12*, 1657–1665. [[CrossRef](#)]
149. *Hydrophobicity Classification Guide*; 1992 STRI Guide 92/1; Swedish Trans Research Institute: Stockholm, Swedish, 1992.
150. Sun, Q.; Lin, F.; Yan, W.; Wang, F.; Chen, S.; Zhong, L. Estimation of the Hydrophobicity of a Composite Insulator Based on an Improved Probabilistic Neural Network. *Energies* **2018**, *11*, 2459. [[CrossRef](#)]
151. Berg, M.; Thottappillil, R.; Scuka, V. Hydrophobicity estimation of HV polymeric insulating materials. Development of a digital image processing method. *IEEE Trans. Dielectr. Electr. Insul.* **2001**, *8*, 1098–1107. [[CrossRef](#)]
152. Gao, Y.; Liang, X.; Bao, W.; Li, S.; Wu, C.; Liu, Y.; Cai, Y. Effects of liquids immersion and drying on the surface properties of HTV silicone rubber: Part I-contact angle and surface chemical properties. *IEEE Trans. Dielectr. Electr. Insul.* **2017**, *24*, 3594–3602. [[CrossRef](#)]
153. Kokalis, C.C.A.; Tasakos, T.; Kontargyri, V.T.; Siolas, G.; Gonos, I.F. Hydrophobicity classification of composite insulators based on convolutional neural networks. *Eng. Appl. Artif. Intell.* **2020**, *91*, 103613. [[CrossRef](#)]
154. Moghadam, M.K.; Taheri, M.; Gharazi, S.; Keramati, M.; Bahrami, M.; Riahi, N. A study of composite insulator aging using the tracking wheel test. *IEEE Trans. Dielectr. Electr. Insul.* **2016**, *23*, 1805–1811. [[CrossRef](#)]
155. Haddad, G.; Wong, K.L.; Petersen, P. Evaluation of the aging process of composite insulator based on surface characterisation techniques and electrical method. *IEEE Trans. Dielectr. Electr. Insul.* **2016**, *23*, 311–318. [[CrossRef](#)]
156. Zhou, Y.; Tu, Y.; Liu, D.; Chen, J.; Wang, C.; Li, R.; Zhang, F.; Zou, L.; Peng, Q. Aging characteristic at different depths in a single composite insulators shed. *IEEE Trans. Dielectr. Electr. Insul.* **2015**, *22*, 1630–1635. [[CrossRef](#)]
157. Chen, J.; Tu, Y.; Chen, C.; Zhang, H.; Xu, Z. Fundamental study of TSC characteristics of RTV coating. In Proceedings of the 2012 International Conference on High Voltage Engineering and Application, Shanghai, China, 17–20 September 2012.
158. Zhang, H.; Tu, Y.; Lu, Y.; Chen, J.; Chen, C.; Xie, L. Influence of the electric field on TSC characteristics of 110kV silicone rubber insulator sheds in service. In Proceedings of the 2012 IEEE International Symposium on Electrical Insulation (ISEI), San Juan, PR, USA, 10–13 June 2012.
159. Wang, Z.; Jia, Z.D.; Jiao, J.K.; Guan, Z.C. Influence of water, NaCl solution, and HNO₃ solution on high-temperature vulcanized silicone rubber. *IEEE Trans. Dielectr. Electr. Insul.* **2016**, *23*, 1164–1173. [[CrossRef](#)]
160. Liang, Y.; Gao, L.J.; Dong, P.P.; Gao, T. The Quantitative Evaluation of Aging State of Field Composite Insulators Based on Trap Characteristics and Volume Resistivity-Temperature Characteristics. *J. Electr. Eng. Technol.* **2018**, *13*, 1355–1362.
161. Tu, Y.; Zhang, H.; Xu, Z.; Chen, J.; Chen, C. Influences of Electric-Field Distribution Along the String on the Aging of Composite Insulators. *IEEE Trans. Power Deliv.* **2013**, *28*, 1865–1871. [[CrossRef](#)]
162. Bi, M.; Yang, J.; Chen, X.; Jiang, T.; Pan, A.; Dong, Y. The Research on Corona Aging Silicone Rubber Materials' NMR Characteristics. *IEEE Access* **2020**, *8*, 128407–128415. [[CrossRef](#)]
163. Xu, Z.; Ye, Q. Optimal Design of a Portable Arc-Shaped NMR Sensor and Its Application in the Aging-Level Detection of Silicone Rubber Insulator. *Appl. Magn. Reson.* **2016**, *47*, 175–189.
164. Zhijin, Z.; Tian, L.; Xingliang, J.; Chen, L.; Shenghuan, Y.; Yi, Z. Characterization of Silicone Rubber Degradation Under Salt-Fog Environment with AC Test Voltage. *IEEE Access* **2019**, *7*, 66714–66724. [[CrossRef](#)]
165. Rowland, M.S. Electrical and material characterization of field-aged 400 kV silicone rubber composite insulators. *IEEE Trans. Dielectr. Electr. Insul.* **2010**, *17*, 375–383. [[CrossRef](#)]
166. Liu, G.; Wu, S.; van de Ven, M.; Molenaar, A.; Besamusca, J. Characterization of Organic Surfactant on Montmo-rillonite Nanoclay to Be Used in Bitumen. *J. Mater. Civ. Eng.* **2010**, *22*, 794–799. [[CrossRef](#)]
167. Sundararajan, R.; Mohammed, A.; Chaipanit, N.; Karcher, T.; Liu, Z. In-service aging and degradation of 345 kV EPDM transmission line insulators in a coastal environment. *IEEE Trans. Dielectr. Electr. Insul.* **2004**, *11*, 348–361. [[CrossRef](#)]
168. Chakraborty, R.; Reddy, B.S. Studies on high temperature vulcanized silicone rubber insulators under arid climatic aging. *IEEE Trans. Dielectr. Electr. Insul.* **2017**, *24*, 1751–1760. [[CrossRef](#)]

169. Chen, C.; Jia, Z.; Wang, X.; Lu, H.; Guan, Z.; Yang, C. Micro characterization and degradation mechanism of liquid silicone rubber used for external insulation. *IEEE Trans. Dielectr. Electr. Insul.* **2015**, *22*, 313–321. [[CrossRef](#)]
170. Jiang, H.; Li, B.; Zhao, B.; Sun, Q.; Gao, C.; Chen, L. Evaluation of aging process of silicone rubber composite insulators with photothermal radiometry. *J. Phys. D Appl. Phys.* **2018**, *51*, 425304. [[CrossRef](#)]
171. Jiang, H.; Li, B.; Zhao, B.; Sun, Q.; Lu, R.; Chen, B. Photothermal Radiometry Depth-Profiling of Aged Silicone Rubber Composite Insulators. *IEEE Trans. Power Deliv.* **2020**, *36*, 3223–3230. [[CrossRef](#)]
172. Jiang, H.; Li, B.; Zhao, B.; Wang, Y. Aging characterization of 500-kV field-serviced silicone rubber composite insulators with self-normalized photothermal radiometry. *Infrared Phys. Technol.* **2021**, *116*, 103763. [[CrossRef](#)]
173. Zhao, W.; Xu, M.; Cheng, X.; Zhao, Z. An Insulator in Transmission Lines Recognition and Fault Detection Model Based on Improved Faster RCNN. *IEEE Trans. Instrum. Meas.* **2021**, *70*, 1–8. [[CrossRef](#)]
174. Zhang, D.; Liu, X.; Yang, C.; Ni, L.; Huang, X.; Zhang, C. Study on the Lifespan Prediction of Silicon Rubber Nanocomposites Under High Humidity and High Temperature Environment. *Sci. Adv. Mater.* **2020**, *12*, 1469–1475. [[CrossRef](#)]